Linnéuniversitetet
Kalmar Växjö

2022

Master's Thesis

Sustainable Production Patterns for Hydropower Units

Author: Hannington Kayanja
Supervisor: Magnus Perninge and Alexander Svensson Marcial
Examiner: Sven-Erik Sandström
Date: 2023-04-14
Course code: 5ED36E, 30,0 hp
Topic: Master's Thesis in Electrical Engineering
Level: Advanced

Department of Physics and Electrical Engineering
Faculty of Technology

Abstract

Globally, a significant portion of energy comes from hydropower. However, harnessing hydro energy interrupts the natural state of river flows, thus affecting the ecological processes of the surrounding communities. In this thesis, a water level control model is described to sustain a desired head for a hydropower plant despite the nature of the stream flows. A scientific analysis is carried out on the physical set up of a hydropower reservoir via mathematical modelling. The study depicts that the amount of electric power, $P_e(t)$ generated from a specific hydro reservoir is mainly controlled by the current water level, $h(t)$ and its corresponding outflow volumes, $f_{out}(t)$. However, these two variables are largely constrained by the behaviour of the inflow volumes, $f_{in}(t)$. So, by relating the torque-force balance equations of all the dynamic elements involved we develop a mathematical model that maintains a steady water level at sustainable inflow rates. The Routh-Hurwitz stability criterion and the Final Value theorem are applied to decide the PD-control actions that stabilize the system. The penstock cross-sectional area, A_P is varied to attain the correct $f_{out}(t)$ for the desired $h(t)$. The model behaviour is verified using Simulink simulation software. Eventually, the model accounts for hydroelectric power production patterns that depends on the nature of the stream flow rates.

***Keywords**: Automatic control, Hydropower modelling, PD-controller, Sustainable power production, Water level control.*

Acknowledgement

In the first place, I genuinely thank the Swedish Institute (SI) for the scholarship opportunity to advance my career both professionally and academically to a master's level. More so, Linnaeus University along with the various departments have always been excellent in providing a decent learning environment amidst the challenges of a multicultural setting. Exclusively, I greatly appreciate all the Faculties at the Department of Physics and Electrical Engineering. The program coordinator for Renewable Electric Power Systems, Ellie Pieternella Cijvat has been a generous teacher and parent to many of us. I thank you for the wonderful guidance always. In a very special way, I recognize my immediate project supervisors, Magnus Perninge the Associate Prof. of Electrical Engineering at Linnaeus University and Alexander Svensson Marcial for suggesting this valuable thesis topic and ensuring healthy educative assistance to me whenever I feel like. I am so grateful for your brilliant concepts among others.

Table of Contents

1. Introduction

1.1. Background

In the world today, sustainability has become a key topic for discussion and integration in almost all industrial sectors. The main goal is to have the current and future generations enjoy the same resources repeatedly without wastage. The Sustainable Development Goals (SDGs), 2030 results into great challenges to the energy sector to transform power production towards sustainability amidst the growing energy demands due to growing populations around the world. Hydropower is a renewable source of electricity that has the potential to balance its production as well as the production of other variable renewable sources like wind and solar through damming and storing water in the reservoirs. It is one of the world's most used sources of electricity [6], [8]. It is expected that the global hydropower generation will raise by 85% by 2050 aiming to decarbonize the globe by substituting fossils with hydropower [6]. Nevertheless, since hydropower production uses water as a key resource to drive the turbines, hydropower producers employ reservoirs to provide hydraulic heads to facilitate electricity generation.

In addition, a water reservoir can be used to release water through the turbines (on schedule) when it's required to balance the energy demands [5], [7]. This is because water reservoirs assist in storing water between seasons of limited flows. More so, reservoirs act as connections between the river flow availability and the energy demand by stocking and storing the required amount of water for electricity production throughout the year. In turn, they introduce artificial water-level changes which alter the natural flow rate of the river due to the numerous fragmentations along the river course. Moreover, the nearby ecological processes and communities are greatly affected [5[, [9]. The Millennium Ecosystem Assessment, 2005 research revealed that of recent days the freshwater ecosystems are among the world's most endangered ecologies [5]. Thus, such environmental impacts need to be alleviated to preserve the environment for both the current and future generations.

In Sweden, about 2000 hydropower plants are installed around the country accounting for an average annual energy production of 65 TWh. This is based on calculations made for periods between 1960–2010 [7]. All such power stations are supposed to undergo environmental rehabilitation through implementing the EU Water Framework Directive (Directive 2000/60/EC) [7]. This is because during the development of river regulations, ecological effects were less considered, where migration paths and minimum flow releases are lacking in most dams [5], [6]. Consequently, new advancements to improve the ecological conditions are equally required. In most cases, hydropower producers would want to implement environmental preservation measures while maintaining their productivity high in the industry.

One of the Swedish regulations set aside to companies operating hydro power stations is that they are required to breed fish to compensate for the damaged breeding grounds around the dam [15]. For instance, at Stornorrfors dam, Vattenfall has set up one of the largest fish-breeding plants (located at Norrfors) [15]. Vattenfall harvests 80,000 salmon smolt, 20,000 sea trout and 20,000 graylings fish annually [15]. In the same spirit, the Vindelälven Fish Council and the Swedish University of Agricultural Sciences have partnered with Vattenfall to analyse how the passage of fish past Stornorrfors can be improved [15].

Thus, in this study, we develop a control model that can be adopted to improve and balance the ecosystem's health around the dam by controlling the water level of the reservoir to a desired height based on the nature of the inflows. We start by examining the water flow data trends of Sweden and then select a sample population to be used in validating the model subsequently. The criteria used to select data was based on location and the annual energy production per installed power capacity on a specific river. Table 1.1 describes some streams in Sweden along with their installed capacities. Lule River located in the Northern part of Sweden, serves the 1st and 3rd largest power stations in Sweden; Harsprånget and Porjus power station with 977 MW and 480 MW installed capacities respectively. It also accommodates the first remotely monitored station (Ligga). In addition,

Umea River serves the 2nd largest power station in Sweden; Stornorrfors power station with 599 MW installed capacity.

Table 1.1: Swedish rivers and installed capacities [9], [15], [16].

Sr.	River name	River length (miles)	Installed power capacity (MW)	Energy production capacity (TWh)
1	Lule älv	460	4117	13,4
2	Indals älv	430	2111	8,5
3	Ångerman älv	460	2599	6,8
4	Ume älv	465	1765	6,8
5	Ljusnan älv	440	817	4,8
6	Dal älv	540	1156	5,6
7	Skellefte älv	440	1017	3,9
8	Fax älv	400	2599	3,5
9	Göta älv	750	303	2,1
10	Ljungan älv	400	602	2,1
11	Klara älv		388	1,9

The installed power stations on such rivers were also sampled to have details of different reservoir information like the water heads and base area estimates. Table 1.2 depicts a list of 10 power plants built along Lule River with their corresponding water heads.

Table 1.2: Hydropower plants in Lule River, Sweden [9], [15].

Sr.	Power plant	River(basin)	Electricity Capacity (MW)	Head (m)
1	Akkats	Lesser Luleälven	157	46
2	Parki	Lesser Luleälven	19	14
3	Laxede	Luleälven	207	25
4	Porsi	Luleälven	282	33
5	Boden	Luleälven	80	13
6	Porjus	Stora Luleälven	417	60
7	Letsi	Lesser Luleälven	483	135
8	Seitevare	Lesser Luleälven	214	182
9	Harsprånget	Stora Luleälven	818	107
10	Ligga	Stora Luleälven	342	40

Thus, based on such samples above we display some flow data below graphically in Figure 1.1. The figure shows the mean monthly water flow rates, [17] that were

measured at Porjus Power station along River Lule in the North of Sweden during the year 2020. From the graph, it's clear that the flow rate follows a trend that depends on the nature of seasons throughout the year. Due to snow melting and high rainfall, the flows increased during the months of January, February and continued into March. Spring floods occurred around early April, thus an increase in the flow rates throughout this period. The flow rates started to decrease from May to July. A rapid flow rate rise kicked off between July and August. This was probably due to the melting snow that remained especially in the mountain areas. The high precipitations during the months of September through into November maintained relatively high flow rates during these months.

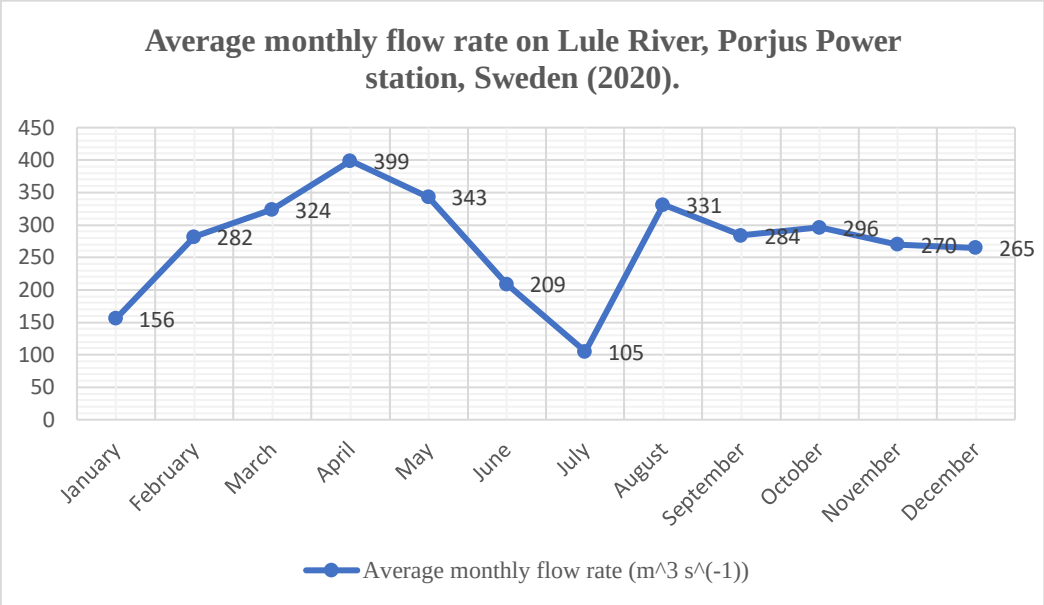

Figure 1.1: Lule River average monthly flow rate [17], [25].

Using the sample flow data pattern above, we later derive a likely production pattern for hydropower units from the plant.

In summary, the model is demonstrated using Simulink software with such hydro flow data collected from Lule River at Porjus Power plant, Sweden. Findings are presented in the results section of this report.

1.2. Problem

Hydropower plants require water reservoirs to suitably facilitate their power generation throughout the year. To fill up a reservoir, often the flow and direction of natural rivers are altered. In most cases, power plants interrupt the water flow by stocking reservoirs basing on seasons, for instance spring through to winter. This disrupts the ecological characteristic of the streams, thus harming dependent habitats. Eventually, it causes a decline in biodiversity around the affected regions. Moreover, in situations of unpredictable extreme rainfalls and melting snow seasons where the stream flow rates are considerably high, the reservoirs attain higher water levels that may result to unnecessary overflows and consequently floods the environs. This may lead to excessive damages to the affected communities. On the other hand, low flow rates may not support the necessary hydropower production.

Further, the Swedish Agency for Marine and Water Management is expected to impose new rules to improve ecological balance [10], [19]. Besides, the EU Water Framework Directive came into force to maintain good ecological and chemical status of water [5]. In this situation, hydropower plants are required to adapt new production models to achieve such green targets. Otherwise, they may face legislative complexity to keep the plants running.

Therefore, in this thesis we design a water level control system model that is aimed at regulating water level in the reservoir to the desired operating level based on the nature of the stream flow. The model is meant to maintain a steady hydro level in the reservoir without interfering with the natural flow behavior of the stream. This is done by manipulating the volume of water that leaves the reservoir to the turbine house depending on what ecologically flows into the reservoir. As a result, we derive a sustainable power production trend that follows the natural flow behavior of the stream, thus reducing damage to the river ecosystems. This will create a smooth bridge between power producers and environmental organizations. This model may be especially suitable for small-scall hydropower plants.

1.3. Purpose

The thesis is aimed at designing a suitable water level control model that can facilitate a green production trend for hydroelectric power units based on the availability of ecological river flows.

1.4. Objectives

The following write up highlights the specific objectives of this thesis work.

- To review related literature and understand in detail different types of controllers as regards to automation and control engineering.
- To identify the water flow mode pattern of Sweden and gather the relevant river flow data.
- To retrieve suitable parameters from river flow data for use in the model validation process.
- To derive the dynamic system equations and hence transfer functions for each dynamic element through the set values to the measured value.
- To establish a controller that can generate a suitable optimized control signal to the actuator to enable system stability.
- To estimate periodic green production patterns for hydroelectric power units of a power plant that is controlled to maintain a steady hydro level for the reservoir.
- To simulate the model, validate it with actual data and acquire results in form of Simulink block diagrams and graphs.
- To document all the findings of this thesis in a report format for future references.

1.5 Methodology

Based on literature review of automation and control theory, hydroelectric power production, and environmental flows, we design a suitable water level control model for a hydroelectric power reservoir. System transfer functions were modelled using mathematical tools like differential equations (DEs) and Laplace transforms to link the system dynamics from set values to the measured values. Moreover, the study of control theory in a more detailed approach provided us

with skills to decide the corresponding parameters for implementing the controller design via the approaches of the Routh-Hurwitz stability criterion and the Final Value theorem.

The samples of water flow data and reservoir information from two major rivers, the Lule River and Umea River of Sweden, were collected using secondary data sources such as SMHI, the Swedish Meteorological and Hydrological Institute and Vattenfall, a Swedish multinational power company that generates power. Mean values from such statistics was utilized to simulate and verify the model via Simulink software. A report detailing the model design and results was presented with block diagrams and graph formats here in.

1.6 Scope of the work

The study is limited to the dynamics of the water reservoir amidst other elements that make up the power plant. We focus on the reservoir inflow and outflow analysis while keeping factors like temperature among others constant. A rectangular cross-sectional area is assumed as the inlet to the penstock. Further, it is assumed that there is no energy loss along the penstock passage to the turbines. All energy at the mouth of the penstock entry is directly transferred to the turbine blades, thereby accounting to a total plant efficiency of around 95%. Moreover, the actuator is implemented with a non-flexible connection shaft to the load. This means that the motor rotor and the load experience equal displacements whenever they happen. Porjus power station water flow information was used as input data to the model. The same data is limited to a measure resolution of mean monthly values. Yet, water heads are actual reservoir heights from the sampled power stations of Porjus power station, Harsprånget power station among others.

2. Theory

2.1 Hydropower

The phrase hydro is a scientific word used in the field of hydrology to mean 'water'. The fall, movement, and circulation of water both on and below the earth's surface is a continuous natural cycle of water known as the water cycle. This water cycle is constantly renewed by the sun and other natural processes. Which means that, if this natural water cycle is not interrupted, water-energy will continue to be available for conversion to other forms of energy especially electric energy, E_e by both the current and the future generations, hence a sustainable energy source.

Creating a dam not only stores and supplies huge volumes of water but also creates an elevation from which water is dropped along a steep pipeline, the penstock to the turbine blades installed in the powerhouse. At the water head, the accumulated water volumes include potential energy, E_p due to the height difference between the head and the tail race just after the powerhouse. The giant penstock (normally round cross-section area of 2–3-meter diameter) provides a column of water with a force directed to the turbine blades via the nozzle (end of the penstock). Figure 2.1 displays a basic schematic configuration of a hydroelectric power plant.

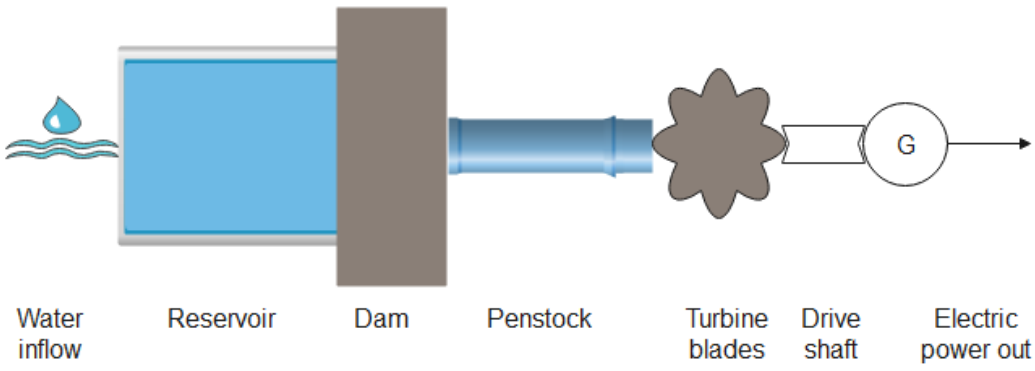

Figure 2.1: Basic schematic set up of a hydroelectric power plant (top view).

The water stored in the reservoir has potential energy. It is this potential energy that is converted to kinetic energy, E_k (with a high velocity) as it flows out of the reservoir via the penstock to the turbine buckets. In turn, the blades rotate the drive

shaft connected to the electricity generator thereby changing the water kinetic energy into mechanical energy, E_m. Furthermore, the rotational mechanical energy is changed to electrical energy, which is then transformed by transformers to higher voltage values for transmission, distribution, and consumption. Figure 2.2 depicts the stages and energy forms involved in converting water energy to electricity energy.

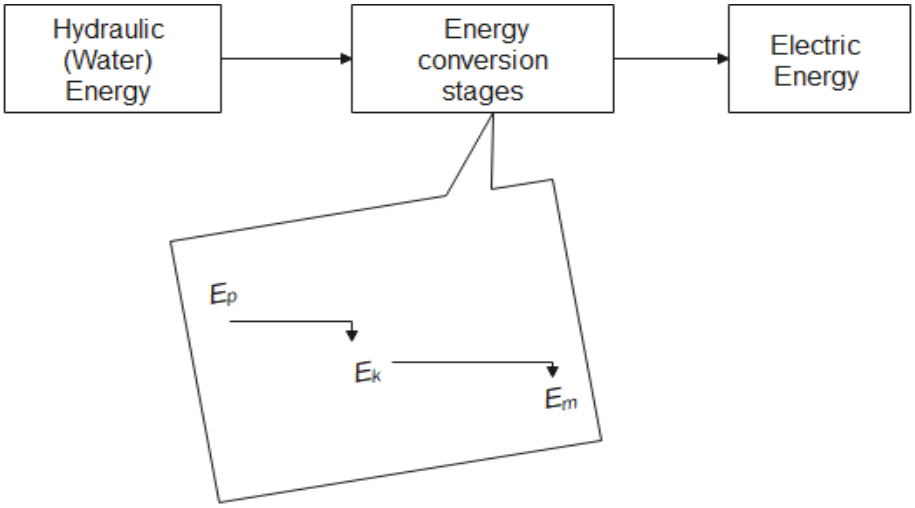

Figure 2.2: Hydro-to-Electric energy conversion block diagram.

2.2 The three-term control actions

In feedback control systems, the fundamental concept is to control and minimize the error signal between the set value and the measured value to an acceptable quantity if not zero. Thus, one can employ at least one form of standard feedback controllers readily available, for instance, the Proportional (P-only), Proportional-Integral (PI), Proportional-Derivative (PD) and Proportional-Integral-Derivative (PID) controllers. The implementation of any of the control modes above depends on the process operating conditions as well as performance requirements. The controller is used to calculate and provide a control (manipulated) signal to the actuator. The signal manipulation is based on how much the system output is offset from the set point. It is not straight forward to choose a particular type of controller to be used. This is because each term responds differently to the error signal. Therefore, one can carry out analysis through some of the available standard

design techniques like Routh-Hurwitz stability criterion [3], Nyquist stability criterion [3], [12], Pole placement [12], [14] among other techniques. Such practices can ease the process of determining specific responses of control terms to the error signal, thereby tuning the controller to a suitable combination. In this thesis, we utilize the Routh-Hurwitz stability criterion which checks whether the roots of the closed loop characteristic equation are in the right half-plane or in the left half-plane and hence derive the range in which the gain values lie for system stability. Moreover, the Final value theorem is also employed to determine steady state errors for each controller combination. Most commonly, a P-only controller is examined first. This is done to ensure that the correction to the controlled variable is relative to the error between the measured value and the desired value. Once this error is acceptable for control, the other control terms are added to the proportional term one by one (if not all at once) to account for the resulting poor system behavior likely to occur during the P-term tuning. Consider the general control system block diagram in Figure 2.3. By assuming an ideal sensor in the negative feedback path, each control term is elucidated further in the next section.

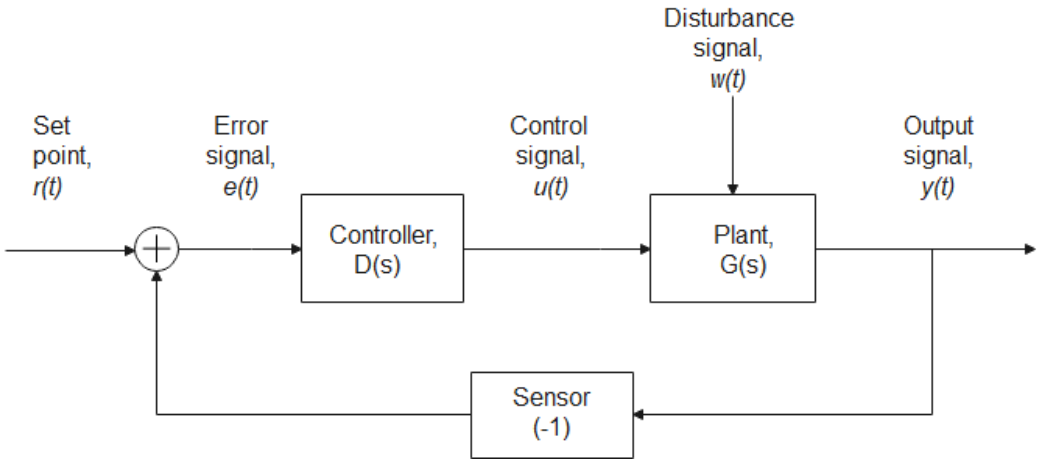

Figure 2.3: General control system block diagram.

2.2.1 The Proportional (P) term

In feedback control, the P-term is supposed to close the feedback loop for the system thereby tracking the reference signal (set point) closely [4]. It is considered the main driving force of the controller [13]. The P-term produces a control signal, $u(t)$ that is proportional to the present error, $e(t)$ between the set value and the

plant output [3]. In other words, $u(t)$ is the controller gain multiplied by $e(t)$ plus a bias [13]. The bias is required to make the resultant control signal a non-zero value once $e(t)$ is zero. Hence, based on this we establish (2.1). In most cases, the bias is neglected in the expressions but considered during implementations.

$$u(t) = k_p\, e(t) \tag{2.1}$$

$where,$

$$k_p = proportional\ gain\ constant$$

Thus, transforming this expression (2.1) to Laplace can support in deriving the controller transfer function further down.

$$U(s) = k_p\, E(s)$$

$$\frac{U(s)}{E(s)} = D(s) = k_p \tag{2.2}$$

It should be noted that a higher gain value results into a higher system output. This may cause the system to oscillate and hence unstable. If k_p is very low, the control action may be very low in response to disturbances. In essence, all these actions could lead to an offset between the set value and actual output value [4], [13]. The offset value is a steady error retained by the controller proportional control action. This is the major drawback of using the P-only control and it cannot correct this problem alone. You must call upon other control terms to eliminate this offset.

2.2.2 The Integral (I) term

This is a control mode, where the control signal $u(t)$ is linearly proportional to the integral of the error signal, $e(t)$. This control term forces the error to zero by considering the past system responses [2]. This implies that $u(t)$ is a sum of all the past tracking errors at each instance the controller is deriving the control signal [3], [4]. We note that, the integral term is not just proportional to the present $e(t)$ but also considers the past errors (if any) cumulatively. This implies that a pure integrator considers both the P-term plus the I-term. This in turn accounts for the constant disturbance cancellation [3]. On the other hand, the response to accumulated past errors can cause the present value to overshoot the set point. So, if the process variable is not at the set value, the integral controller will continue to change the controller output until the error is zero. Of course, you must give

adequate time to this control term to carry out the control action sufficiently. Therefore, from this information we define the $I-term$ mathematically in (2.3) below.

$$u(t) = k_i \int_0^t e(\tau)\, d\tau \tag{2.3}$$

$where,$

$$k_i = integral\ gain\ constant$$

$$\tau = variable\ of\ integration\ that\ takes\ on\ values\ of\ t$$

$$= 0\ to\ the\ current\ time, t$$

If we transform (2.3) to the $s-domain$, the following transfer function for the integral term is obtained.

$$U(s) = k_i\ \frac{E(s)}{s}$$

$$\frac{U(s)}{E(s)} = D(s) = \frac{k_i}{s} \tag{2.4}$$

For small errors, the integral term will increase or reduce the value of the control signal at a slow rate. If $e(t)$ is large, the controller output will be changing at faster rates. The controller's integral time, τ sets the speed of the integral action [13]. A longer τ results in a slow integral action and vice versa.

2.2.3 The Derivative (D) term

The third and final control term is the derivative term, where the control law suggests that $u(t)$ is proportional to the time derivative of $e(t)$ [3]. That is, it looks at the present rate of change of the error as expressed below in (2.5).

$$u(t) = k_d \frac{d}{dt} e(t) \tag{2.5}$$

$where,$

$$k_d = derivative\ gain\ constant$$

Expression (2.5) can be transformed into Laplace to obtain the controller transfer function below in (2.6).

$$U(s) = k_d\ sE(s)$$

$$\frac{U(s)}{E(s)} = D(s) = k_d\ s \tag{2.6}$$

It should be noted that, the $D-term$ improves the system closed loop stability, speeds up transient response, and reduces overshoots [3]. The most important feature of this controller is that it predicts where the future error is heading [2], thereby giving a control action based on the $e(t)$ behavior. Thus, leaving other factors constant the design engineer has control over the three controller constant gains (k_p, k_i and k_d) only, which he/she can modify to achieve a suitable control signal to the process under control.

2.3 Motors

In most cases, various types of direct current (DC) motors like shunt motors, compound motors and series motors are applied as primary movers depending on the load connections, type of loads, amount of starting torque, among others. For instance, the load can be connected directly to the motor shaft or through a gear arrangement [18]. More so, the load can be constant or intermittent. Thus, in this thesis a typical DC motor is selected to provide a translational motion to the outflow gate valve. However, the motor theory is partially covered by this thesis: (see section 4.1).

3. Electric power from a hydropower plant

In this section, we specifically examine and derive expression that can evaluate the amount of electric power from a given water reservoir set for generation of hydropower units.

3.1 The instantaneous electric power from a given hydropower reservoir

The electric power, P_e in joules per second or watts can be expressed as a function of the present water level difference, h and the corresponding amount of water, f_{out} exiting the reservoir at a certain time. That is, $P_e = f(h, f_{out})$. Thus, given the volumetric outflow rate (m^3/s) of water, the head (m), installed capacity (MW) and the efficiency of the plant, the amount of electricity to be generated can be determined. This can be derived from the gravitational potential energy, E_p (which depends on mass and vertical position of the object) present in the volumes of water contained in the reservoir at a particular time, t. Hence, referring to Figure 3.1 below we assume a water reservoir of base area, A_r (m^2) and the penstock aperture area, A_p (m^2). The theoretical P_e is obtained and henceforth decide the actual by involving the overall plant efficiency. We let the average total weight of the water body to be at the centre of gravity (c.g).

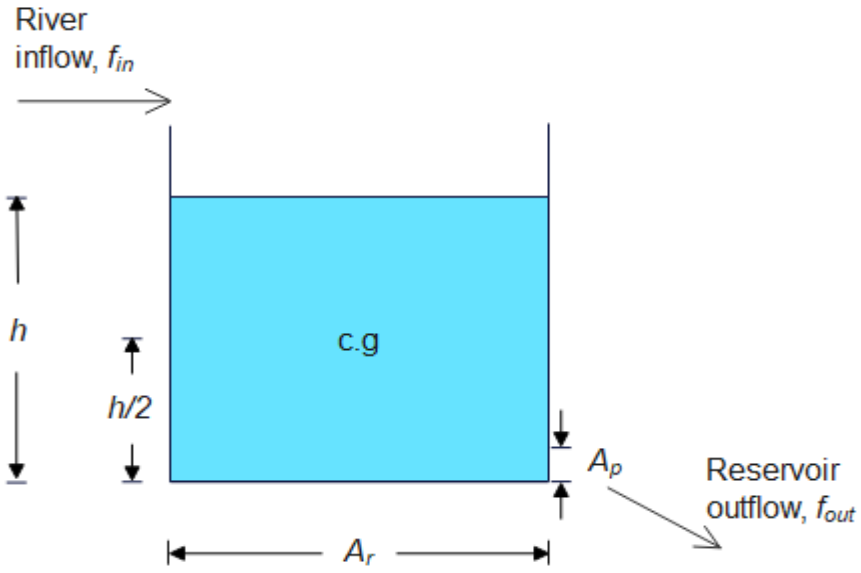

Figure 3.1: Hydropower reservoir water inflow and outflow relationship.

We start by noting the energy-balance fact that electrical energy, E_e is equal and opposite to the corresponding potential energy, E_p currently available in the reservoir. In other words, as we extract E_e from the moving or falling water of the reservoir, E_p reduces in the reservoir. Hence,

$$\delta E_e = -\delta E_p \tag{3.1}$$

And from definition, power is the rate of change of energy. Therefore, the theoretical instantaneous electrical power available in the falling water from any given reservoir can then be expressed as the *time derivative* of the present potential energy in the reservoir. This leads us to (3.2) below.

$$P_e = \frac{d}{dt}(-E_p) \tag{3.2}$$

Also, there are some energy losses along the energy conversion process which reduce the practical P_e to some value less than the theoretical P_e. This means that the system efficiency, η must be well-thought-out to account for these losses. Hence equation (3.3) results.

$$P_e = \eta \frac{d}{dt}(-E_p) \tag{3.3}$$

Then, from (3.3) we need to obtain E_p since this is the present potential energy in the volume of water contained by the reservoir. Thus, using the formula for gravitational potential energy, we assume a water body of mass m elevated against the gravitational force, $F = mg$ to an elevation of height, h. Then, the potential energy in (3.4) results.

$$E_p = mgh \tag{3.4}$$

If we consider c.g to act at half the height, the average potential energy of the water in the reservoir will be as defined below in (3.5).

$$E_p = mg\left(\frac{h}{2}\right) \tag{3.5}$$

Then, considering the definition of the total mass of water contained in the reservoir, we get the following derivation in (3.6).

$$E_p = (\rho \delta V)g\left(\frac{h}{2}\right) = (\rho A_r h)g\left(\frac{h}{2}\right) = \rho A_r g\left(\frac{h^2}{2}\right) \tag{3.6}$$

where,

g = The acceleration due to gravity (ms^{-2})

ρ = The density of water (kgm^{-3})

Therefore, we now substitute for E_p, (3.6) in (3.3), which turn out to be (3.7) as described below.

$$P_e = \eta \frac{d}{dt}\left(-\rho A_r g\left(\frac{h^2}{2}\right)\right)$$

$$= -\left(\eta \frac{1}{2}(\rho A_r g)\right)\frac{d}{dt}(h^2)$$

$$= -(\eta \rho A_r g) h \frac{dh}{dt}$$

$$\Rightarrow \qquad P_e = -(\eta \rho A_r g) h\dot{h} \tag{3.7}$$

If we apply the continuity relation governing fluid flow [2], the rate of change of height can be given by equation (3.8).

$$\dot{h} = \frac{(f_{in} - f_{out})}{A_r} \tag{3.8}$$

where,

f_{in} = Volumetric inflow rate $(m^3 s^{-1})$

f_{out} = Volumetric outflow rate $(m^3 s^{-1})$

Since the final power is only influenced by the amount of water flowing out of the reservoir instantaneously, the volumetric inflow rate, f_{in} tends to zero at that instant. Hence, the rate of change of the reservoir water level (3.8) becomes (3.9)

$$\dot{h} = \left(\frac{-f_{out}}{A_r}\right) \tag{3.9}$$

The negative sign implies that the flow rate reduces with decrease in height. Substituting (3.9) in (3.7), we get (3.10) as described below.

$$P_e = -(\eta \rho A_r g) h \left(\frac{-f_{out}}{A_r}\right)$$

$$\therefore \qquad P_e = \eta \rho g (h f_{out}) \tag{3.10}$$

Consequently, the practical P_e is a function of the current water level difference, h and the total present volume, f_{out} of water exiting a given reservoir through a guided path, the penstock. That is, $P_e = f(h, f_{out})$.

4. System mathematical modelling and design

In this section, we develop mathematical models for the three main dynamic elements interconnected within the water level control system for a hydropower water reservoir. That is, the motor, water valve and water reservoir. The model for the expected P_e is also obtained herein. Each dynamic element has a specific DE that explains its dynamics. The idea of the DEs model dynamic phenomena is to support in determining the various system dynamic equations that describe the dynamics of each subsystem from the input voltage, v_a to the resultant water level, h. Thus, the transfer functions of the dynamic elements can be obtained by relating the DEs with Laplace transforms. We start by providing an illustration of the intended set up of the hydropower reservoir, Figure 4.1. A DC motor is connected to the water valve to provide it with translational motions.

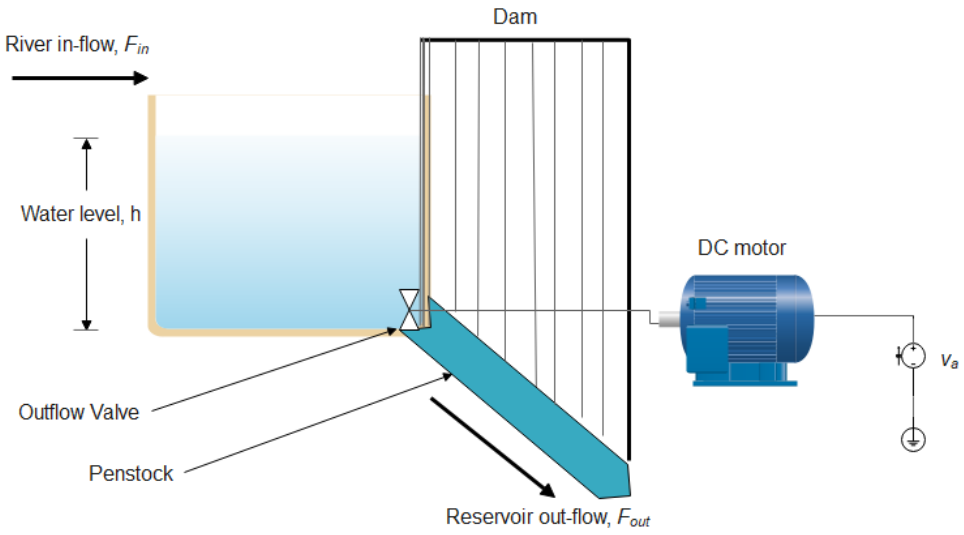

Figure 4.1: Simplified schematics for a motor-controlled hydropower water reservoir.

The motor has the ability to move in both clockwise and anticlockwise rotational motions. In this model we use an armature controlled DC motor to control the position, x of the outflow valve by rotating the connected shaft in either direction. Figure 4.2 illustrates the physical system model as a simplified block diagram of two subsystems.

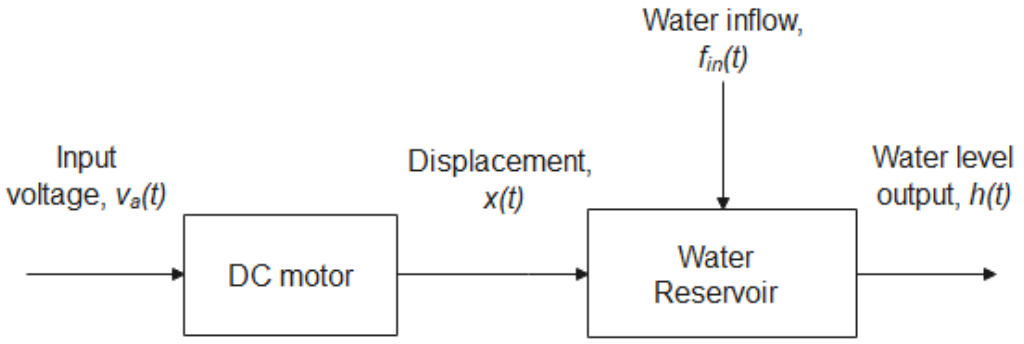

Figure 4.2: Block diagram for the motor controlled water reservoir.

We consider natural water inflows as disturbances to the water reservoir and the main control objective of the model is to maintain the water level at the desired height. This is because, a height too high may produce an overflow to the reservoir hence unsafe and height too low may not support the anticipated production of hydropower units. The water reservoir operation is assumed to be continuous throughout the year depending on the availability of the natural hydro intake rates. Thus, the water reservoir is the process under control. It should be noted that the manipulated variables depend on the existing input variables to the process. There are two types of control strategies that can be employed here: The feed-back controller and the feed-forward controller. The feed-back controller is designed to measure the output of the process and compares it with the desired value while the feed-forward controller measures the disturbance inputs and sends them to the controller to tune the manipulated variable to an acceptable performance of the control system before it's too late [2]. It should be noted that there are various benefits related to the feedforward control strategy, for instance disturbance is measured and allows immediate correction to be done before it affects the reservoir level. However, in this model only feed-back control strategy is considered. This is detailed in Figure 4.3 below.

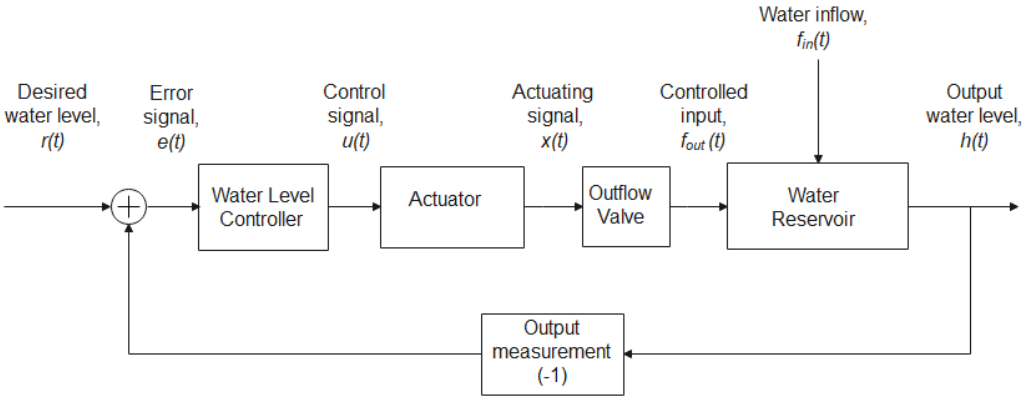

Figure 4.3: Detailed block diagram showing dynamic elements interconnecting the intended water level control system model for a hydropower reservoir with manipulated outflow volumes.

Each dynamic element relates a particular output to a specific input within the system. That is, the reservoir section relates f_{out} to the overall system output, h, the level controller relates the resultant error, e between the desired height and the measured height to the control signal, u and the actuator relates u to the actuating signal, x, which in turn translates to f_{out}. The assumption is that the output measurement is done perfectly with zero errors, so we can neglect the transfer function of the measurement element in the closed loop set up.

4.1 The system dynamic equations describing the motor

In general, we consider an armature equivalent electrical circuit and load connections, Figure 4.4. A control signal (voltage source) is applied to the armature windings which in turn induce an electro motive force (back emf), e_{coil}. The emf is proportional to the rotary motion velocity, $\dot{\theta}_r = \dot{\theta}$ of the shaft by the electrical constant, K_e [4]. There is a motor torque, T_m generated by the DC motor. This torque is also proportional to the armature current by the torque constant, K_t [4].

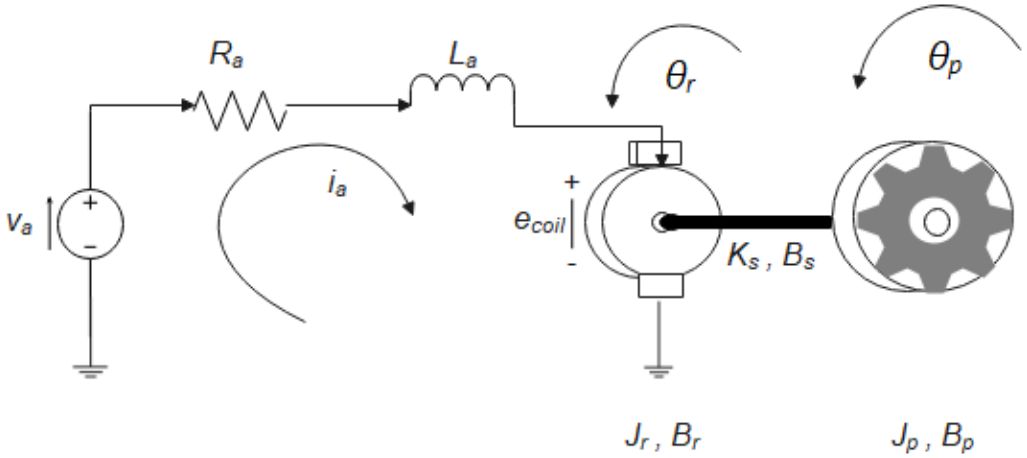

Figure 4.4: The armature equivalent electrical circuit and the connected load.

Hence, based on the above description the following coupling equations are true.

$$e_{coil} = K_e\dot{\theta} \tag{4.1}$$

$$T_m = K_t i_a \tag{4.2}$$

Also, we use Kirchhoff's voltage law (2nd law) to sum up all the voltages around the loop. We can as well call it the voltage balance equation.

$$L_a\frac{di_a}{dt} + i_a R_a = v_a - K_e\dot{\theta} \tag{4.3}$$

In many cases, the relative effect of the inductance is negligible compared with the mechanical displacements, hence neglecting the armature inductance, L_a [3]. Thus, (4.3) becomes (4.4).

$$i_a R_a = v_a - K_e\dot{\theta} \tag{4.4}$$

Applying Laplace transform, (4.4) can be expressed in the s-domain as below.

$$R_a I_a(s) = V_a(s) - K_e s\Theta(s) \tag{4.5}$$

4.2 The system dynamic equations describing the rotor

In principle, the rotational motion is governed by Newton's 2nd law of motion, $F = ma$. Therefore, the total moment, M about the point is equal to the product of the body's mass moment of inertia, I about the same point and its acceleration, $\ddot{\theta}$ [2], [3]. It should be noted that a non-flexible shaft is assumed, thereby leading to the same angle of rotation, $\theta_r = \theta_p = \theta$ for both the rotor and the pinion gears. This leads us to equation (4.6).

$$M = I\ddot{\theta} \tag{4.6}$$

4.2.1 The torque balance equations: Rotary motion

As earlier highlighted, a non-flexible shaft connection between the motor rotor and the load (the valve system) is considered, Figure 4.5. So, the shaft spring constant, K_s and viscous damping, B_s values are negligible ($K_s = B_s = 0$). This implies that the angular rotation of the rotor is equally transferred to the connected load, the pinion gear.

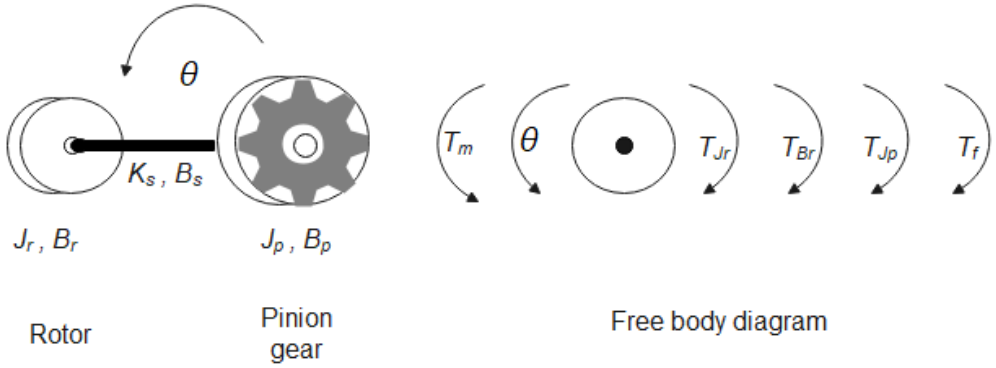

Figure 4.5: The physical rotor, the load and free body diagram.

Therefore, the following definitions are considered from [2], [4].

T_m = Motor torque proportional to the armature current, i_a

$$T_m = K_t i_a$$

T_{J_r} = Opposing torque due to rotor inertia, J_r

= proportion to angular acceleration, $\ddot{\theta}$

$$T_{J_r} = J_r\ddot{\theta}$$

T_{B_r} = Opposing torque due to viscous friction, B_r around the rotor

= proportion to angular velocity, $\dot{\theta}$

$$T_{B_r} = B_r\dot{\theta}$$

T_{J_p} = Opposing torque due to load (pinion gear) inertia, J_p

= proportion to angular acceleration, $\ddot{\theta}$

$$T_{J_r} = J_p\ddot{\theta}$$

T_f = Opposing torque due to the force, $f(t)$ exerted by the pinion gear to the rack gear as it rotates

$= force\ x\ perpendicular\ distance$

$$T_f = r_p f(t)$$

$$where, r_p = radius\ of\ the\ pinion\ gear$$

Hence, based on Newton's 2nd law of motion stated above, $\sum T = 0$ we sum up all the torques acting on the system to get (4.7)

$$T_m - \left(T_{J_r} + T_{B_r} + T_{J_p} + T_f\right) = 0$$

$$K_t i_a - \left(J_r \ddot{\theta} + B_r \dot{\theta} + J_p \ddot{\theta} + r_p f(t)\right) = 0 \quad (4.7)$$

If we rearrange and apply Laplace transform, (4.7) can be expressed in s-domain as in (4.8).

$$J_r s^2 \Theta(s) + B_r s\Theta(s) + J_p s^2 \Theta(s) + r_p F(s) = K_t I_a(s)$$

$$\left(J_r s^2 + J_p s^2 + B_r s\right)\Theta(s) + r_p F(s) = K_t I_a(s) \quad (4.8)$$

4.3 The system dynamic equations describing the valve

A rectangular valve of horizontal length, l, connected in rack and pinion gear arrangement is considered, Figure 4.6 with gear ratio of $1:1$. The figure also includes the free body diagram showing the forces experienced by the sliding gate due to the force exerted by the pinion gear. Moreover, a balancing weight is assumed hanging at the opposite side of the sliding gate to balance the gravitational force, $F_g = M_g g$ where M_g is the mass of the sliding gate. This indicates that the force due to gravitational acceleration is also ignored from the final translational equations of motion.

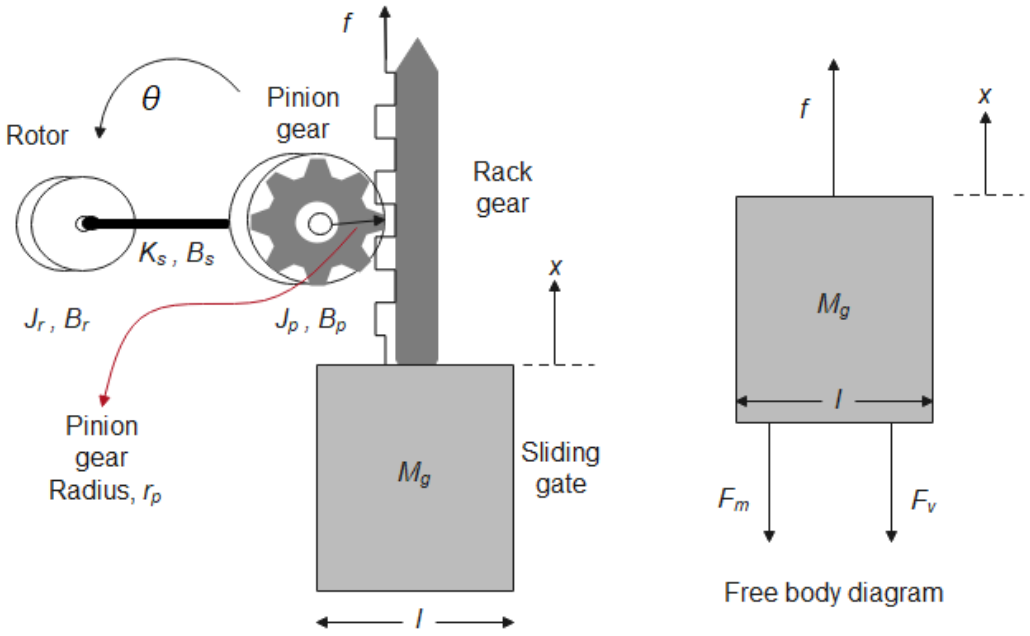

Figure 4.6: The physical structure of the outflow valve system and a free body diagram.

The setup of the rack and pinion gears converts angular displacements into linear motions. This arrangement will cause the valve to move vertically in either direction thereby allowing less or more volumes of water out of the reservoir. The rotation, θ rads of the pinion gear provides a linear displacement, x meters in the rack gear attached to the valve. Therefore, we must consider the two motions. This is illustrated in equation (4.9) and (4.10) further down.

$$r_p\theta = x \tag{4.9}$$

And using Laplace transform, we get (4.10)

$$r_p\,\Theta(s) = X(s) \tag{4.10}$$

It should be noted that equation (4.10) is the coupling expression for the motor with the valve system by translating the rotor motion into a valve displacement.

4.3.1 The force balance equations: Translational motion

The pinion gear exerts a force on the rack to enable it to move in either direction. As a reaction, the rack (and the valve) exerts a force, f which is equal in magnitude and opposite in direction to the force exerted by the pinion gear. The following forces are realised as shown on the free body diagram of figure 4.6 above.

f = Pinion force equal and opposite to rack force

F_m = Opposing force due to valve inertia, M_g

= proportion to translational acceleration, $\ddot{x}$

$$F_m = M_g\ddot{x}$$

F_v = Opposing force due to viscous friction around the valve, B_g

= proportion to translational velocity, $\dot{x}$

$$F_v = B_g\dot{x}$$

Therefore, from Newtons 2nd law of motion stated above, $\sum F = 0$. We sum up all the forces acting on the valve to get (4.11).

$$f - (F_m + F_v) = 0$$

$$f(t) - \left(M_g\ddot{x} + B_g\dot{x}\right) = 0 \quad (4.11)$$

If we rearrange and apply Laplace transform, (4.11) can be expressed in the s-domain as in (4.12).

$$F(s) - \left(M_g s^2 X(s) + B_g sX(s)\right) = 0$$

$$F(s) = \left(M_g s^2 + B_g s\right)X(s) \quad (4.12)$$

4.4 The system dynamic equations describing the water reservoir

We consider the rate of change of the water level in equation (3.8) as the continuity relation governing the fluid flow in the reservoir. This is recalled as below.

$$\dot{h} = \frac{(f_{in} - f_{out})}{A_r}$$

Since we intend to control f_{out} in this model, we define the volumetric flow rate out of the reservoir by the following expression.

$$f_{out} = A_p v \quad (4.13)$$

where,

v = velocity (ms^{-1}) of water as it leaves the reservoir.

To find the velocity of water leaving the reservoir bottom, we employ Bernoulli's equation: The principle of conservation of energy relates pressure, p, velocity, v,

(kinetic energy), height, h, (potential energy) of any two points in a flowing fluid of density, ρ [15].

$$p + \frac{1}{2}\rho v^2 + \rho g h = constant \tag{4.14}$$

So, for the water reservoir under consideration, we name the topmost water surface as point-1 and point-2 at the out-flow valve of the water reservoir, Figure 4.7.

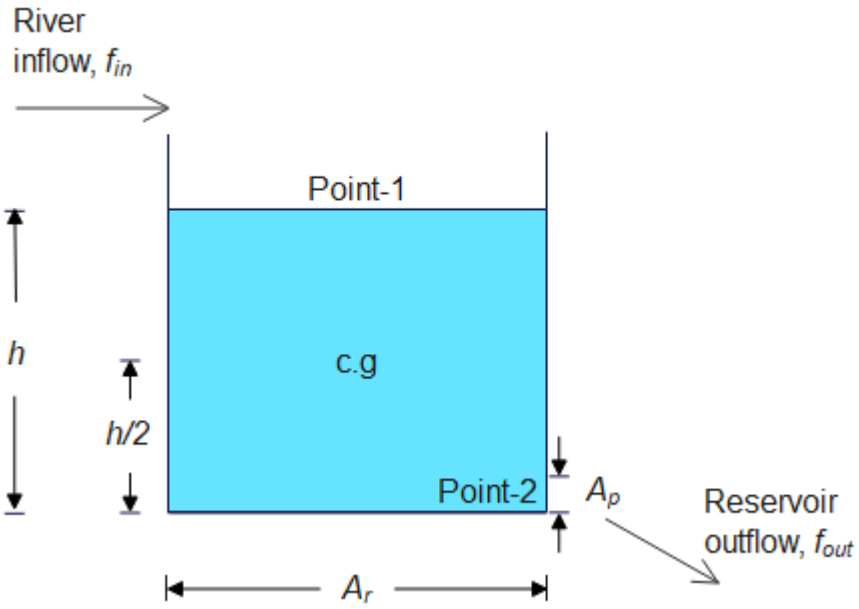

Figure 4.7: Two reference points considered in the water reservoir.

If we apply equation (4.14) to these two selected points, the following expression results.

$$p_1 + \frac{1}{2}\rho v_1^2 + \rho g h_1 = p_2 + \frac{1}{2}\rho v_2^2 + \rho g h_2 \tag{4.15}$$

The following assumptions should be noted:

- Both points 1 and 2 are exposed to atmospheric pressure, p_a. Hence, $p_1 = p_2 = p_a$.
- The water at point-2 is moving much faster than the water at point-1. Hence, $v_1 \ll v_2$ implying that $v_1 \approx 0$.

Applying these assumptions in (4.15), we rearrange and get the expression for the velocity of water at point 2.

$$g h_1 = \frac{1}{2} v_2^2 + g h_2$$

$$v_2 = \sqrt{2gh} \tag{4.16}$$

$where,$

$$h = (h_1 - h_2)$$

Therefore, substituting for the velocity, v of water in (4.13) we get the following expression.

$$f_{out} = A_p v = A_p\sqrt{2gh} = xl\sqrt{2gh} \quad (4.17)$$

By replacing f_{out} in formula (3.8) for rate of change of water level above, we arrive at (4.18).

$$\dot{h} = \frac{1}{A_r}\left(f_{in} - l\sqrt{2g}.x\sqrt{h}\right) \quad (4.18)$$

Equation (4.18) above describes the dynamics of the water reservoir. It's a non-linear dynamic equation in terms of h. At this point, we cannot proceed to take any Laplace transform for this kind of equation since it is a non-linear DE. However, we can carry out linearisation on this non-linear term by various methods like Taylor series expansion, Jacobian linearization that involves evaluating matrices of partial derivatives at the equilibrium points, among others [4], [21], [23]. For this model, we utilize Taylor series method.

4.4.1 Linearization of the non-linear DE for the water reservoir

The dynamic system equation (4.18) is clearly a non-linear equation that describes the reservoir outflow that depends upon the product of the valve displacement, x and the square root of the present water level, h. If we consider three variables of h, x and f_{in} changing as a function of time. It implies that $h(t), x(t)$ and $f_{in}(t)$ is true. Therefore, by Taylor series let $\dot{h} = f(h, x, f_{in})$.

$$\Rightarrow \quad f(h,x,f_{in})$$

$$= f\left(h_0,x_0,f_{in_0}\right) + \frac{\partial f}{\partial h}(h,x,f_{in})\underset{\substack{h=h_0\\x=x_0\\f_{in}=f_{in_0}}}{at,} (h-h_0)$$

$$+ \frac{\partial f}{\partial x}(h,x,f_{in})\underset{\substack{h=h_0\\x=x_0\\f_{in}=f_{in_0}}}{at,} (x-x_0)$$

$$+ \frac{\partial f}{\partial f_{in}}(h,x,f_{in})\underset{\substack{h=h_0\\x=x_0\\f_{in}=f_{in_0}}}{at,} \left(f_{in}-f_{in_0}\right) \tag{4.19}$$

From expression (4.18),

$$\dot{h} = f(h,x,f_{in}) = \frac{1}{A_r}(f_{in} - l\sqrt{2g}.x\sqrt{h}) \tag{4.20}$$

Then, by applying the equilibrium point conditions in (4.20), the terms in (4.19) can be defined explicitly as follows.

$$f\left(h_0,x_0,f_{in_0}\right) = \frac{1}{A_r}\left(f_{in_0} - x_0 l\sqrt{2gh_0}\right)$$

And the partial derivatives.

$$\frac{\partial f}{\partial h}(h,x,f_{in})\underset{\substack{h=h_0\\x=x_0\\f_{in}=f_{in_0}}}{at,} .(h-h_0) = \frac{-x_0 l\sqrt{2g}}{2A_r\sqrt{h_0}}(h-h_0)$$

$$\frac{\partial f}{\partial x}(h,x,f_{in})\underset{\substack{h=h_0\\x=x_0\\f_{in}=f_{in_0}}}{at,} .(x-x_0) = \frac{-l\sqrt{2gh_0}}{A_r}(x-x_0)$$

$$\frac{\partial f}{\partial f_{in}}(h,x,f_{in})\underset{\substack{h=h_0\\x=x_0\\f_{in}=f_{in_0}}}{at,} .\left(f_{in}-f_{in_0}\right) = \frac{1}{A_r}\left(f_{in}-f_{in_0}\right)$$

Then, replacing all these partial derivatives in (4.19)

$$f(h,x,f_{in}) = \frac{1}{A_r}\left(f_{in_0} - x_0 l\sqrt{2gh_0}\right) + \frac{1}{A_r}\left(f_{in}-f_{in_0}\right) - \frac{l\sqrt{2gh_0}}{A_r}(x-x_0)$$

$$- \frac{x_0 l\sqrt{2g}}{2A_r\sqrt{h_0}}(h-h_0) \tag{4.21}$$

Now, if we consider steady state conditions it implies none of the state is changing.

$$\therefore \qquad \dot{h} = f(h, x, f_{in}) = 0$$

Then, by using these conditions in equations (4.21) we prove that (4.22) is true.

$$0 = \frac{1}{A_r}\left(f_{in_0} - x_0 l\sqrt{2gh_0}\right)$$

$$f_{in_0} = x_0 l\sqrt{2gh_0} \tag{4.22}$$

Substituting for f_{in_0} in (4.21), we get (4.23)

$$f(h, x, f_{in}) = \frac{1}{A_r}\left(x_0 l\sqrt{2gh_0} - x_0 l\sqrt{2gh_0}\right) + \frac{1}{A_r}\left(f_{in} - f_{in_0}\right)$$

$$- \frac{l\sqrt{2gh_0}}{A_r}(x - x_0) - \frac{x_0 l\sqrt{2g}}{2A_r\sqrt{h_0}}(h - h_0)$$

$$f(h, x, f_{in}) = \frac{1}{A_r}\left(f_{in} - f_{in_0}\right) - \frac{l\sqrt{2gh_0}}{A_r}(x - x_0)$$

$$- \frac{x_0 l\sqrt{2g}}{2A_r\sqrt{h_0}}(h - h_0) \tag{4.23}$$

We can now convert equation (4.23) into deviation, $\partial(.)$ variables to reproduce (4.24). Thus, let

$$\partial h = (h - h_0) \qquad \Rightarrow \dot{\partial h} = \dot{h} = f(h, x, f_{in})$$

$$\partial x = (x - x_0)$$

$$\partial f_{in} = \left(f_{in} - f_{in_0}\right)$$

Then,

$$\dot{\partial h} = \left(\frac{1}{A_r}\right)\partial f_{in} - \left(\frac{l\sqrt{2gh_0}}{A_r}\right)\partial x - \left(\frac{x_0 l}{2A_r}\sqrt{\frac{2g}{h_0}}\right)\partial h \tag{4.24}$$

This can be written further down as,

$$\dot{H} = \left(\frac{1}{A_r}\right)F_{in} - \left(\frac{l\sqrt{2gh_0}}{A_r}\right)X - \left(\frac{x_0 l}{2A_r}\sqrt{\frac{2g}{h_0}}\right)H$$

$$\dot{H} = \left(\frac{1}{A_r}\right)\left(F_{in} - \left(l\sqrt{2gh_0}\right)X - \left(\frac{x_0 l}{2}\sqrt{\frac{2g}{h_0}}\right)H\right) \tag{4.25}$$

It is at this stage that we have a linear dynamic equation, (4.25) describing the dynamics of the hydro reservoir in terms of inflow disturbance, f_{in}, displacement x, of the outflow valve, and the final water level, h. If we now apply Laplace transform to (4.25), the subsequent expression, (4.26) known as the transfer function from both $X(s)$ and $F_{in}(s)$ to $H(s)$ of the reservoir is obtained as follows.

$$sH(s) = \left(\frac{1}{A_r}\right)F_{in}(s) - \left(\frac{l\sqrt{2gh_0}}{A_r}\right)X(s) - \left(\frac{x_0 l}{2A_r}\sqrt{\frac{2g}{h_0}}\right)H(s)$$

$$sH(s) + \left(\frac{x_0 l}{2A_r}\sqrt{\frac{2g}{h_0}}\right)H(s) = \left(\frac{1}{A_r}\right)F_{in}(s) - \left(\frac{l\sqrt{2gh_0}}{A_r}\right)X(s)$$

$$\left(s + \left(\frac{x_0 l}{2A_r}\sqrt{\frac{2g}{h_0}}\right)\right)H(s) = \left(\frac{1}{A_r}\right)F_{in}(s) - \left(\frac{l\sqrt{2gh_0}}{A_r}\right)X(s) \qquad (4.26)$$

4.5 The system dynamic equation describing the electric power

This can easily be derived by further defining the parameters for (f_{out}) in (3.10) by using the known parameters.

$$P_e = \eta\rho g h f_{out}$$

In the above equation, we replace f_{out} with its definition from (4.17). The following is obtained.

$$P_e = \eta\rho g h\left(xl\sqrt{2gh}\right)$$

$$\therefore \qquad P_e = \eta\rho l g^{\left(\frac{3}{2}\right)}\sqrt{2}\left(xh^{\left(\frac{3}{2}\right)}\right) \qquad (4.27)$$

Expression (4.27) describes the dynamics for the expected electric power generated based on the natural hydro intakes.

5. Simulation of system dynamics using differential equations

In this section, we rewrite the DEs that explains the dynamics of the subsystems connecting the overall model. This is achieved by use of the system dynamic equations developed in the previous sections. These are collectively summarized below.

$$R_a I_a(s) = V_a(s) - K_e s\Theta(s) \tag{4.5}$$

$$\left(J_r s^2 + J_p s^2 + B_r s\right)\Theta(s) + r_p F(s) = K_t I_a(s) \tag{4.8}$$

$$r_p\, \Theta(s) = X(s) \tag{4.10}$$

$$F(s) = \left(M_g s^2 + B_g s\right)X(s) \tag{4.12}$$

$$\left(s + \left(\frac{x_0 l}{2A_r}\sqrt{\frac{2g}{h_0}}\right)\right)H(s) = \left(\frac{1}{A_r}\right)F_{in}(s) - \left(\frac{l\sqrt{2gh_0}}{A_r}\right)X(s) \tag{4.26}$$

5.1 The motor subsystem

Based on the system dynamic equations above, we derive a transfer function for the input voltage, $v_a(t)$ to the motor through angular displacement, $\theta(t)$ to a translational displacement, $x(t)$ of the outflow valve. It's this transfer function that is converted back to the original DE in the time-domain. The DE is then used to formulate an equivalent Simulink block diagram for simulation purposes using zero initial conditions as follows.

From (4.5), the expression for the armature current, $I_a(s)$ is obtained as below.

$$I_a(s) = \left(\frac{V_a(s) - sK_e\Theta(s)}{R_a}\right) \tag{5.1}$$

Then, we substitute for $I_a(s)$ and $F(s)$ in equation (4.8)

$$\left(J_r s^2 + J_p s^2 + B_r s\right)\Theta(s) + r_p F(s) = K_t I_a(s)$$

$$\left(s^2 J_r + s^2 J_p + sB_r\right)\Theta(s) + r_p\left\{\left(s^2 M_g + sB_g\right)X(s)\right\} = K_t\left\{\frac{V_a(s) - sK_e\Theta(s)}{R_a}\right\}$$

$$\left(s^2 J_r + s^2 J_p + sB_r + \frac{sK_t K_e}{R_a}\right)\Theta(s) + \left(s^2 r_p M_g + s r_p B_g\right)X(s)$$

$$= \left(\frac{K_t}{R_a}\right)V_a(s) \tag{5.2}$$

From equation (4.10), we derive the expression for $\Theta(s)$.

$$\Theta(s) = \left(\frac{X(s)}{r_p}\right) \tag{5.3}$$

Therefore, we replace $\Theta(s)$ in equation (5.2) and simplify the resultant expression to (5.4) below.

$$\left(s^2 J_r + s^2 J_p + sB_r + \frac{sK_t K_e}{R_a}\right)\left\{\frac{X(s)}{r_p}\right\} + \left(s^2 r_p M_g + s r_p B_g\right)X(s) = \left(\frac{K_t}{R_a}\right)V_a(s)$$

$$\left\{\left(s^2 J_r + s^2 J_p + sB_r + \frac{sK_t K_e}{R_a}\right)\frac{1}{r_p} + \left(s^2 r_p M_g + s r_p B_g\right)\right\}X(s) = \left(\frac{K_t}{R_a}\right)V_a(s)$$

Multiply through by r_p, we get the following.

$$\left\{\left(s^2 J_r + s^2 J_p + sB_r + \frac{sK_t K_e}{R_a}\right) + \left(s^2 {r_p}^2 M_g + s {r_p}^2 B_g\right)\right\}X(s) = \left(\frac{r_p K_t}{R_a}\right)V_a(s)$$

Now, let's rearrange all the constant parameters in the above expression as coefficients of s. This is rewritten as below.

$$\left\{\left(J_r + J_p + {r_p}^2 M_g\right)s^2 + \left(B_r + {r_p}^2 B_g + \frac{K_t K_e}{R_a}\right)s\right\}X(s) = \left(\frac{r_p K_t}{R_a}\right)V_a(s)$$

$$\left\{\left(J_r + J_p + {r_p}^2 M_g\right)s^2 X(s) + \left(B_r + {r_p}^2 B_g + \frac{K_t K_e}{R_a}\right)sX(s)\right\}$$

$$= \left(\frac{r_p K_t}{R_a}\right)V_a(s) \tag{5.4}$$

In the time domain, we modify the transfer function described by equation (5.4) to a DE in (5.5) and further down making $\ddot{x}(t)$ the subject in (5.6).

$$\left\{\left(J_r + J_p + {r_p}^2 M_g\right)\ddot{x}(t) + \left(B_r + {r_p}^2 B_g + \frac{K_t K_e}{R_a}\right)\dot{x}(t)\right\} = \left(\frac{r_p K_t}{R_a}\right)v_a(t)$$

$$\ddot{x}(t) = \frac{1}{\left(J_r + J_p + {r_p}^2 M_g\right)}\left\{\left(\frac{r_p K_t}{R_a}\right)v_a(t) - \left(B_r + {r_p}^2 B_g + \frac{K_t K_e}{R_a}\right)\dot{x}(t)\right\} \tag{5.5}$$

$$\ddot{x}(t) = (K_1)\{K_2 v_a(t) - K_3 \dot{x}(t)\} \tag{5.6}$$

where

$$K_1 = \left(\frac{1}{\left(J_r + J_p + {r_p}^2 M_g\right)}\right),\ K_2 = \left(\frac{r_p K_t}{R_a}\right) \text{ and } K_3 = \left(B_r + {r_p}^2 B_g + \frac{K_t K_e}{R_a}\right)$$

Considering the zero initial conditions, we use equation (5.6) to construct the Simulink block diagram in Figure 5.1 to reproduce the motor system dynamics for a unity step input voltage.

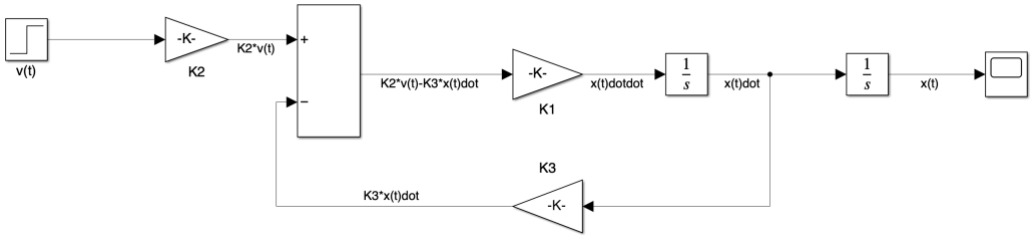

Figure 5.1: Block diagram describing the motor subsystem.

In reference to Section 3.1-page 162 of [4], we suppose that the DC motor has a torque constant, K_t, electrical constant, K_e, and armature resistance, R_a. The motor is connected to a rack and pinion gear system arrangement with effective radius, r_P. The gear system is attached to a rectangular valve of horizontal length, l, vertical length, y, and mass, M_g. Table 5.1 below describes these DC motor and valve specifications in detail. We use them to evaluate the model transfer functions and run the simulation.

Table 5.1: Motor and Valve specifications [3], [4].

Sr.	Description	Name	Value	Units
1	Rotor viscous friction	B_r	*0.01*	$Nmrad^{-1}s^{-1}$
2	Rotor inertia	J_r	*5.00E-05*	kgm^2
3	Electrical constant	K_e	*0.02*	NmA^{-1}
4	Torque constant	K_t	*0.03*	NmA^{-1}
5	Armature resistance	R_a	*10*	*Ohm*
6	Pinion and Track gear effective radius	r_p	*0.1*	*m*
7	Outflow gate valve viscous friction	B_g	*0.02*	$Nmrad^{-1}s^{-1}$
8	Pinion gear inertia	J_p	*2.00E-10*	kgm^2
9	Mass of the outflow gate valve	M_g	*100*	*kg*

On running the simulation, Figure 5.2 displays the motor response in terms of $x(t)$ to a unity step input with respect to time, t. The vertical displacement of the outflow gate increases from around zero towards infinity with either a constant or increasing step input, $v(t)$. After 100 seconds, it's clearly shown that the motor shifts the valve up to 1.1 meters.

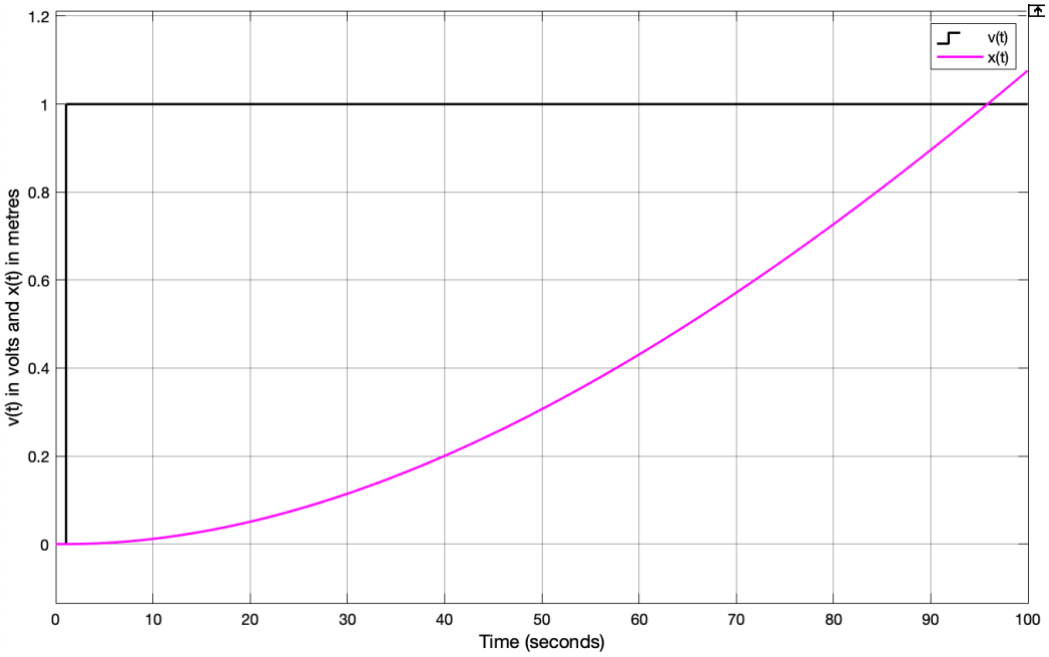

Figure 5.2: The motor response to the step input.

5.2 The hydro reservoir subsystem

The dynamics of the hydro reservoir are described from $x(t)$ to $h(t)$ in two modes. The non-linear dynamic version and the linearized dynamic version. This section explains the dynamics for both categories.

5.2.1 The non-linear hydro reservoir model

We start with the actual scenario of the reservoir by considering expression (4.18) that describes the original reservoir with a non-linear term, $h(t)$. Note that this is already in time domain and may not be transformed to the $t - transform.$

$$\dot{h} = \frac{1}{A_r}\left(f_{in} - l\sqrt{2g}.x\sqrt{h}\right)$$

$$\dot{h}(t) = \left(\frac{1}{A_r}\right)\left(f_{in}(t) - l\sqrt{2g}.x(t)\sqrt{h(t)}\right) \tag{5.7}$$

Which can be expressed below as in (5.8) with constant terms reduced to $K - constants.$

$$\dot{h}(t) = K_4\left(f_{in}(t) - K_5.x(t).\sqrt{h(t)}\right) \tag{5.8}$$

$where,$

$$K_4 = \left(\frac{1}{A_r}\right) \text{ and } K_5 = \left(l\sqrt{2g}\right)$$

For purposes of predicting the variations of the water inflows to the reservoir, a sinusoidal wave form with a unit amplitude is utilized as the disturbance signal. A $bias = 1$ is added to the wave form to shift the curve above the $x - axis$. Figure 5.3 shows the resulting signal.

$$f_{in}(t) = Sin(\omega t + \varphi) + Bias \tag{5.9}$$

$where,$

$$\varphi = phase \text{ and } \omega t = frequency$$

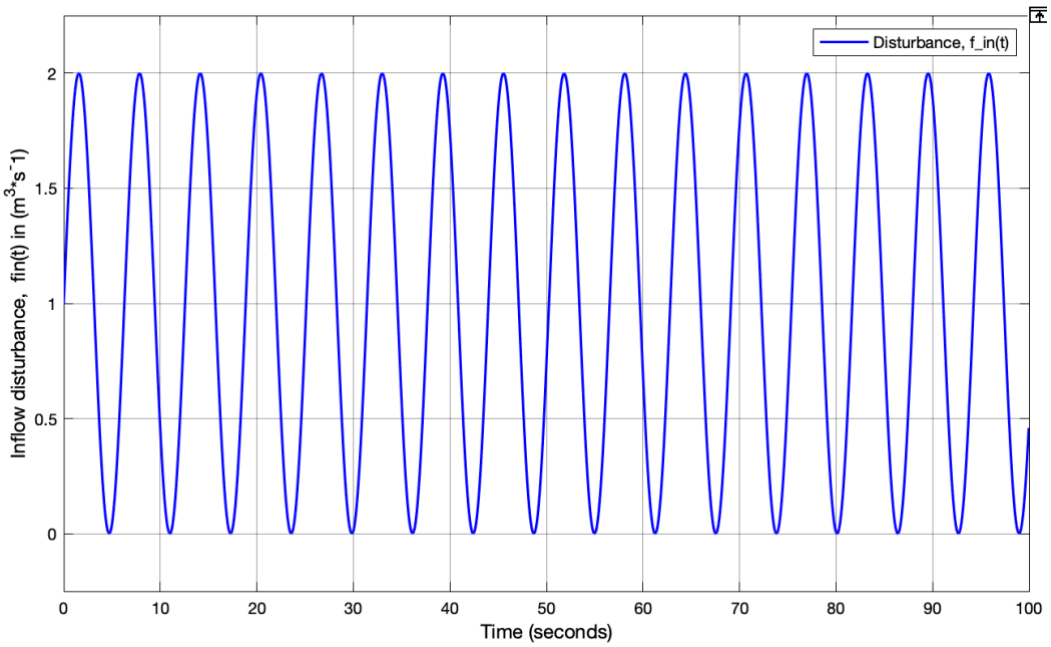

Figure 5.3: Disturbance signal, $f_{in}(t)$.

Therefore, using equation (5.8) above, we build up the Simulink block diagram as shown in Figure 5.4 below.

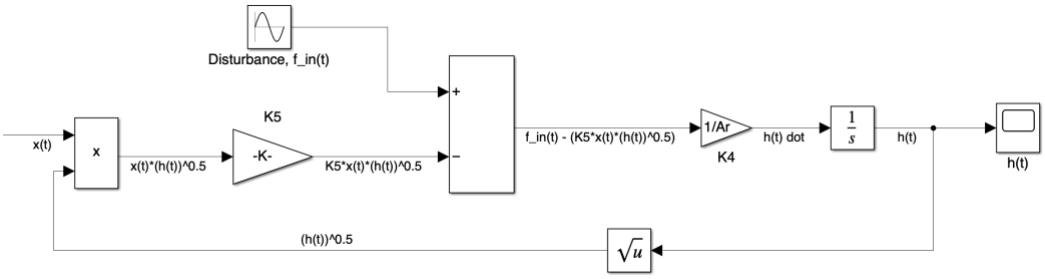

Figure 5.4: Block diagram showing the non-linear water reservoir system.

Table 5.2 shows the average sample values of some of the major hydropower plants in Sweden [9]. Using these parameters as input values to the simulation, we test the dynamics of the non-linear water reservoir system model above in Simulink software. Figure 5.5 displays the response of the reservoir to the valve displacement due to a unity step input voltage to the motor.

Table 5.2: Mean values of sample data for a typical hydro reservoir.

Sr.	Description	Name	Value	Units
1	Reservoir base area	A_b	*1000*	m^2
2	Acceleration due to gravity	g	*9.80665*	ms^{-2}
3	Reservoir operating water level	h_0	*100*	m
4	Outflow gate valve horizontal length	l	*2*	m

Consequently, the resultant output, $h(t)$ is depicted by the following Figure 5.5. The plot shows a clear inverse proportionality of $h(t)$ in the reservoir due to increasing displacement, $x(t)$ of the outflow gate. This is because as the gate opens widely, the water leaving the reservoir increases and so a reduction in the water level is achieved. It's observed that during the first few seconds, the water level is stable at 100 meters because step input is zero at that time. However, as time increases the water level starts to reduce. After $450\ s$ of a constant step input, the water level goes to zero, Figure 5.5 below. This action will continue if there is an input voltage to the motor that keeps the valve open by adjusting x. Hence the reason to explore available controllers to support in optimizing and maintaining the desired system state.

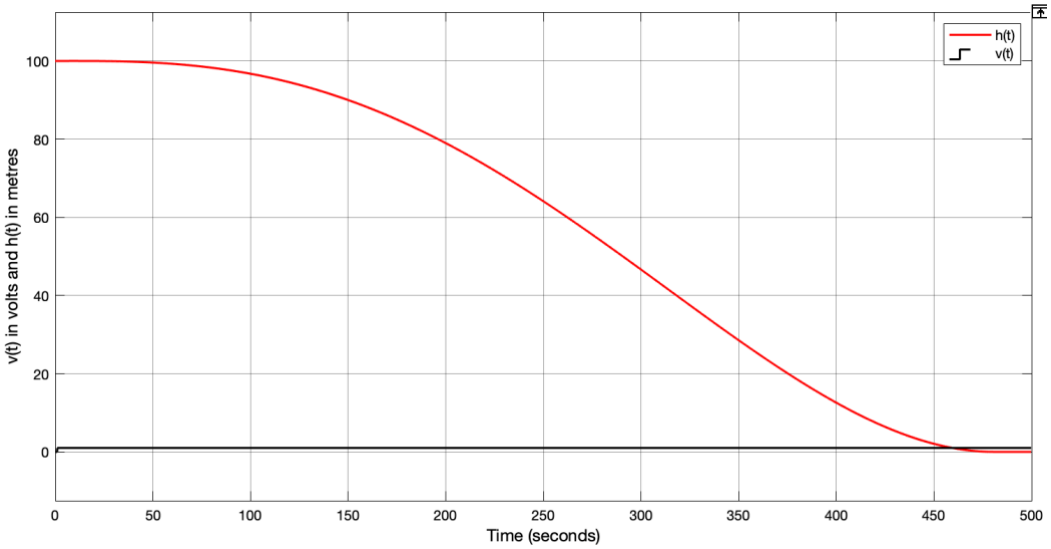

Figure 5.5: Response of the non-linear water reservoir system model to the valve displacement due to a step input voltage.

5.2.2 The linearized hydro reservoir model

Following the linearized system dynamic equation (4.26) for the hydro reservoir, a transformation to time domain is carried out and the relevant Simulink block diagram for the linearized reservoir model is constructed. This is described in the following derivations. Firstly, we convert the equation from $s-domain$ to $t-domain$. It should be noted that when deriving DEs for simulation, it may be easier to make the highest derivative of the target variable the subject. For instance, in this case we are targeting the water level, $h(t)$ so we make its highest derivative the subject.

$$\left(s+\left(\frac{x_0 l\sqrt{2g}}{2A_r\sqrt{h_0}}\right)\right)H(s)=\left(\frac{1}{A_r}\right)F_{in}(s)-\left(\frac{l\sqrt{2g}\sqrt{h_0}}{A_r}\right)X(s)$$

$$sH(s)+\left(\frac{x_0 l\sqrt{2g}}{2A_r\sqrt{h_0}}\right)H(s)=\left(\frac{1}{A_r}\right)F_{in}(s)-\left(\frac{l\sqrt{2g}\sqrt{h_0}}{A_r}\right)X(s)$$

$$sH(s)=\left(\frac{1}{A_r}\right)F_{in}(s)-\left(\frac{l\sqrt{2g}\sqrt{h_0}}{A_r}\right)X(s)-\left(\frac{x_0 l\sqrt{2g}}{2A_r\sqrt{h_0}}\right)H(s)$$

$$\dot{h}(t)=\left(\frac{1}{A_r}\right)f_{in}(t)-\left(\frac{l\sqrt{2g}\sqrt{h_0}}{A_r}\right)x(t)-\left(\frac{x_0 l\sqrt{2g}}{2A_r\sqrt{h_0}}\right)h(t)$$

$$\dot{h}(t) = \left(\frac{1}{A_r}\right)\left(f_{in}(t) - \left(l\sqrt{2gh_0}\right)x(t) - \left(\frac{x_0 l}{2}\sqrt{\frac{2g}{h_0}}\right)h(t) \right) \quad (5.10)$$

Which can be expressed as in equivalence (5.11) below with $K - constants$:

$$\dot{h}(t) = K_4\{f_{in}(t) - K_6 x(t) - K_7 h(t)\} \quad (5.11)$$

$where$

$$K_6 = \left(l\sqrt{2gh_0}\right) \text{ and } K_7 = \left(\frac{x_0 l}{2}\sqrt{\frac{2g}{h_0}}\right)$$

Accordingly, (5.11) provides the basis to develop the Simulink block diagram for the linearized reservoir system model in Figure 5.6.

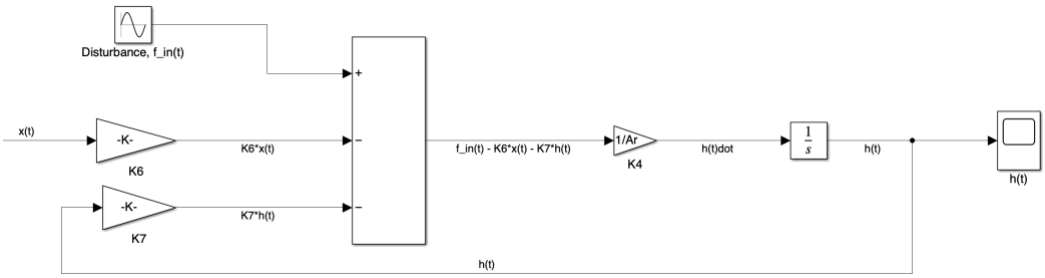

Figure 5.6: Block diagram showing the linearized water reservoir system model.

Again, referring to parameter values in Table 5.1 and 5.2 while maintaining the same disturbance input signal, the dynamic behavior of the linearized reservoir is explored, Figure 5.7. The plot reveals a clear inverse proportionality of the height of water in the reservoir with respect to increasing $x(t)$ of the outflow gate. Approximately, it's the same behavior as in the non-linearized model in Figure 5.5 above. It's observed that the water level starts to drop as soon as the valve opens and its after $340\ s$ that the level goes zero. It will continue to decrease if the motor maintains the valve open. It's noticed that the response in the linearized model is less accurate compared to the non-linearized version probably due to the truncated higher order terms during the linearization process. However, the two models depict the same behavior of inverse proportions of the water level in the reservoir with respect to variations in x due to a step input voltage to the system model.

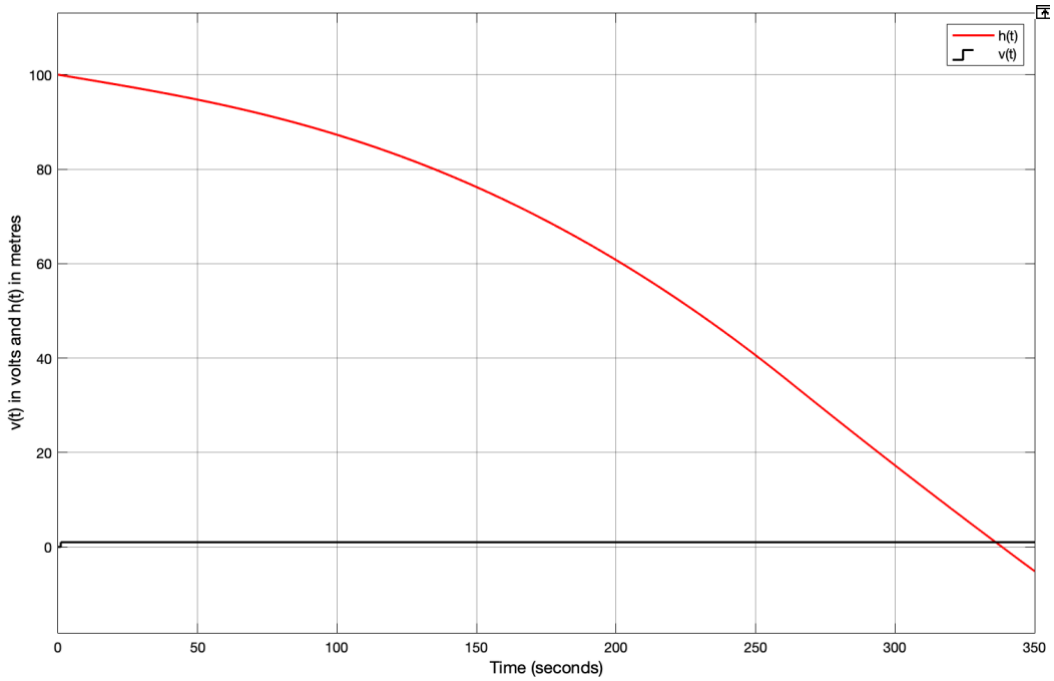

Figure 5.7: Response of the linearized hydro reservoir system model to valve displacement due to a step input to the system model.

5.3 The equilibrium state for the hydro reservoir system model

A system is stable if all its rates of change tend to zero as time tends to infinity. In such situations, there is no change of the system from its operating point(s) and if they so happen, they are negligible. Thus, a steady state condition of the hydro reservoir is achieved. The intention of control system design is to keep the process at a desired state steadily. Therefore, we need to find the equilibrium (critical) points that will make the rates of change go to zero. We start with the non-linearized dynamic system model equation, (5.7). This implies setting the rates of change for the hydro level to zero, $\dot{h}(t) = 0$ and obtain the operating point(s) for the system as follows. That is, the value(s) of $x(t)$ at which the system will be maintained at steady state. Thus,

$$\dot{h} = \left(\frac{1}{A_r}\right)\left(f_{in} - l\sqrt{2g}.x\sqrt{h}\right)$$

$$0 = \left(\frac{1}{A_r}\right)\left(f_{in} - l\sqrt{2g}.x\sqrt{h}\right)$$

$$x = \frac{f_{in}}{\left(l\sqrt{2g}\right)\sqrt{h}} \tag{5.12}$$

Expression (5.12) defines the operating point(s), x of the hydro reservoir system. The value(s) strongly depend on the water inflow, f_{in} and the resultant hydro level, h. The more the inflow into the reservoir, the more the outflow valve is shifted upwards to release more water out of the reservoir to the power generators. This is so to regain and maintain the preferred water level at the steady state. So, in reference to Lule River flow data (Figure 1.3) we suppose an average inflow rate of $f_{in} = 200\, m^3 s^{-1}$ and consider Table 5.2 parameters above, the required operating point(s) can be evaluated as below by using (5.12).

$$x = \frac{200}{2\sqrt{2(9.80665)100}} = 2.258004\, m$$

The above value is the vertical displacement of the outflow gate for which a steady state of the water level is maintained at $h = 100\, m$ in the reservoir given an average water inflow of $200\, m^3 s^{-1}$. This is on the assumption that there are no further disturbances into the system.

Note that at operating point(s), there is no input voltage to the motor since at this point, there is nothing to adjust any further. Hence, the armature voltage, $v_a(t)$ will momentarily level to zero. This means that there is no difference between the desired and actual water level that can influence a change in the valve movement. Therefore, at $t = 0\ s$ all initial conditions are applicable, and the following steps can then be executed in Simulink for both the non-linear and linearized hydro reservoir systems.

- Using a constant Simulink block, we set the desired water level at $h = 100\ m$.
- In the Simulink integration blocks, we set the initial condition values for both the motor valve displacement, x and the water level, h.
- Install a saturation Simulink block and set the maximum displacement to a minimum of twice the operating value (saturation block upper limit parameter is equal to at least twice the equilibrium value, x. That is, $x = 2 \times 2.258$). Note that, it should not be more than the dimensions of the penstock. This will allow the motor to displace the valve within a good range, for instance $0\ to\ 5\ m$.
- Using a Simulink constant block, we set the inflow to an average flow rate of $f_{in} = 200\, m^3 s^{-1}$.

- A unit (negative) feedback is connected between the output and the set point.

This is done to provide a comparison between the response and desired points. At equilibrium, the error between the output and the set point must level to zero. The resultant Figure 5.8 depicts the Simulink block diagram connections for the system model at steady state conditions.

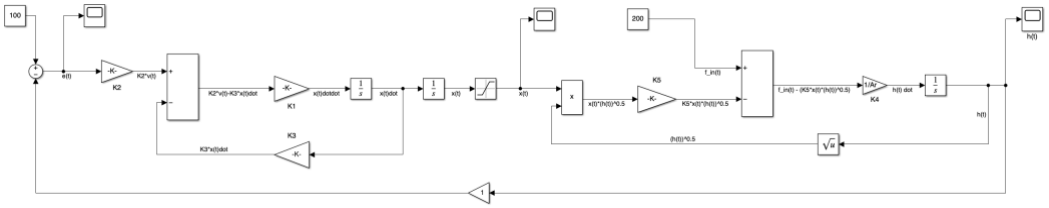

(A)

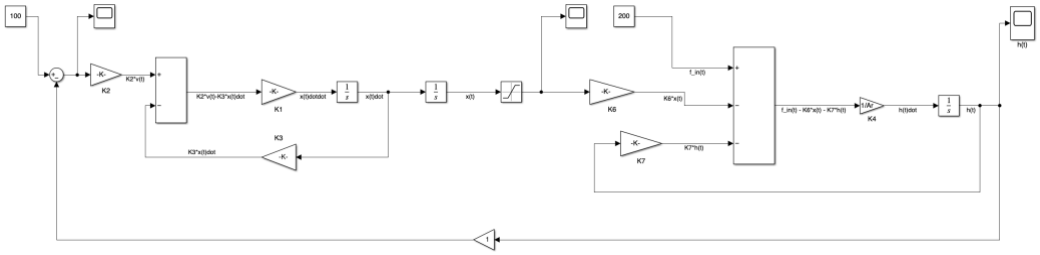

(B)

Figure 5.8: Simulink block diagram connections for the system model at equilibrium; **(A)** the non-linear hydro reservoir system model and **(B)** the linearized hydro reservoir system model.

At this point, we will continue to work with the non-linearized system model going forward since it depicts the real-life scenario. Therefore, Figure 5.9 demonstrates the plots resulting from the above simulations of Figure 5.8(A). At an average flow rate of $f_{in} = 200\, m^3 s^{-1}$, the valve displacement is seen at its equilibrium value of $x(t) = 2.258\, m$, Figure 5.9. The figure includes the plots of the subsequent error signal, $e(t) = 0\, m$ and water level that is retained at the desired level of $h(t) = 100\, m$.

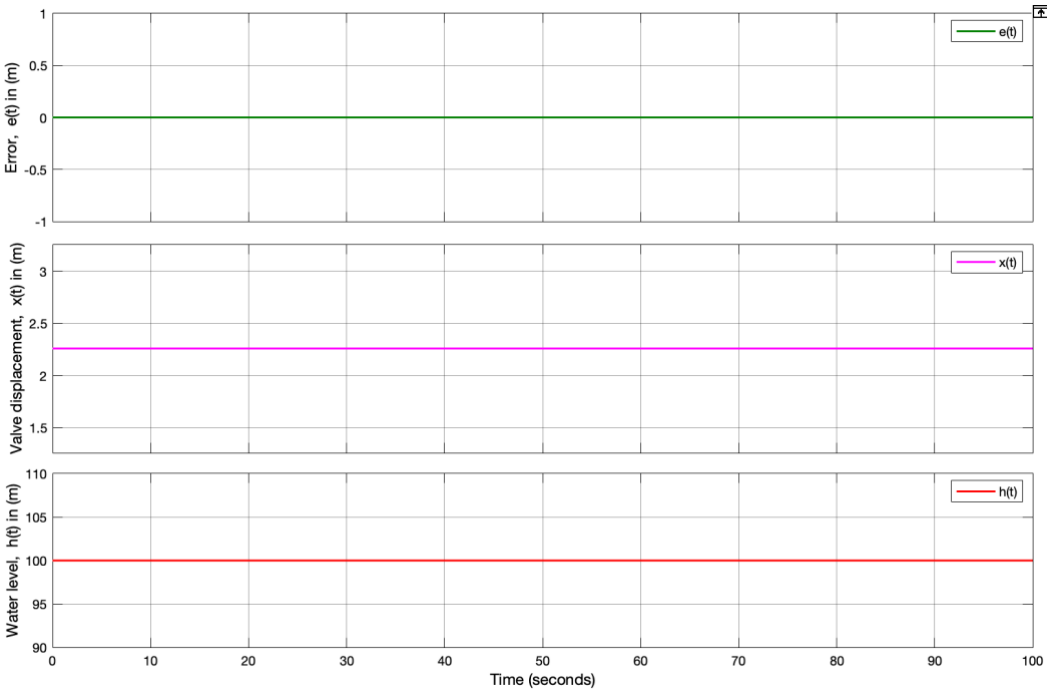

Figure 5.9: System model response at equilibrium; the error signal, valve displacement and water level output respectively.

Now that the system model works steadily at steady state condition. Appropriately, we need to maintain the water level at these chosen operating points to keep a smooth and continuous operation of the hydropower plant. This is because, if any of the operating values are altered to values other than the critical values, the system will become unstable. Meanwhile, there is no way we can stop the perturbations from happening but rather put in place control measures to regulate such unwanted signals into the steady process. Thus, this calls for a control measure that can support the engineers to keep the system at a preferred hydro level which can enable a smooth production for the projected hydropower units. This can be done by designing a standard feedback controller that measures the hydro level output of the reservoir, compares it with the set value and then adjusts the process input signal to attain the required system behavior.

In the next sections, we determine a controller that will produce the required control signal to direct the motor on what action to take. The motor then decides the best size of the outflow passage by varying its cross-section area, A_P that in turn influences the water level at the set point.

6. Selecting the controller

In control systems, control engineers have no standard parameters set for any feedback controller to regulate a given plant, but rather the parameters depend on the process subjected to control. Thus, the engineer must first understand the dynamics of the system end to end and there after use the available techniques to ascertain the correct parameters for specific control actions based on some chosen performance measures. Nevertheless, we need a starting point to be able to start the controller design. Therefore, in reference to Figure 4.3 in Section 4 above we derive a simplified block diagram below in Figure 6.1 to start the design process of the intended controller.

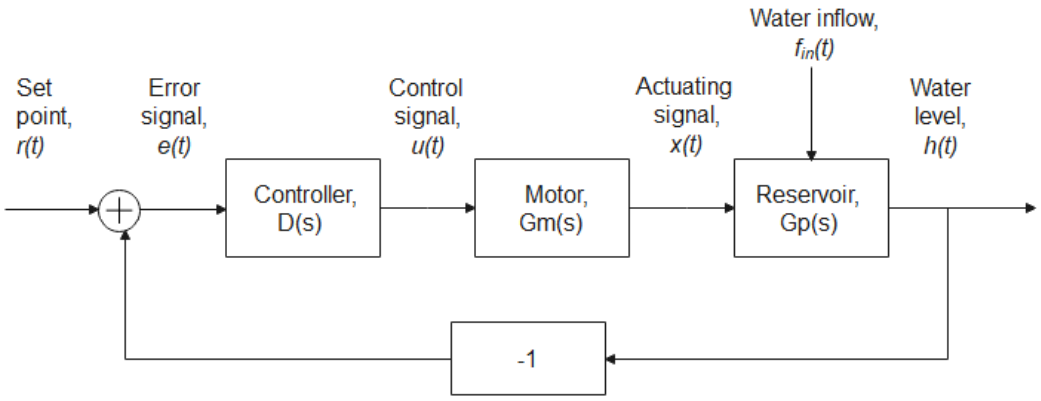

Figure 6.1: The hydro level control system model for a water reservoir.

There are three main dynamic elements that are considered in this model, that is the controller, motor, and the reservoir. Thus, from definition the closed-loop unity feedback transfer function can be obtained as below.

$$\frac{H(s)}{R(s)} = \left(\frac{D(s)G_m(s)G_p(s)}{1 + D(s)G_m(s)G_p(s)}\right) \tag{6.1}$$

where,

$$D(s): Controller\ transfer\ function$$

$$G_m(s): Motor\ transfer\ function$$

$$G_p(s): Reserver\ transfer\ function$$

It follows that, the closed-loop characteristic polynomial is then given by the following expression.

$$1 + D(s)G_m(s)G_p(s) = 0 \tag{6.2}$$

Accordingly, using Routh's stability criterion we can examine the coefficients of equation (6.2). This requires one to evaluate all the transfer functions involved in the expression. In the next section, we define the transfer functions for each of the dynamic elements involved in the planned closed loop system. Soon after, stability will be assessed and then we decide which controller to maintain it for a smooth system operation.

6.1 The system transfer functions

By using the open-loop system approach, the system transfer functions for the main dynamic elements are derived from the system dynamic equations obtained in the previous sections. The overall system is split up into three subsystems, the Controller, Motor, and Hydro reservoir. Note that the transfer functions for standard feedback control terms were dealt with in the literature review section. So, in this section we evaluate the transfer function for the motor and the reservoir models.

6.1.1 The motor subsystem

By re-arranging equation (5.4), we define the open loop transfer function for the motor subsection further down in (6.3).

$$\left\{\left(J_r + J_p + {r_p}^2 M_g\right)s^2 X(s) + \left(B_r + {r_p}^2 B_g + \frac{K_t K_e}{R_a}\right)sX(s)\right\} = \left(\frac{r_p K_t}{R_a}\right)V_a(s)$$

$$\frac{X(s)}{V_a(s)} = \frac{\left(\frac{r_p K_t}{R_a}\right)}{\left\{\left(J_r + J_p + {r_p}^2 M_g\right)s^2 + \left(B_r + {r_p}^2 B_g + \frac{K_t K_e}{R_a}\right)s\right\}}$$

$$\frac{X(s)}{V_a(s)} = \frac{\left(\frac{r_p K_t}{R_a}\right)}{s\left\{\left(J_r + J_p + {r_p}^2 M_g\right)s + \left(B_r + {r_p}^2 B_g + \frac{K_t K_e}{R_a}\right)\right\}} \tag{6.3}$$

Thus, using Table 5.1 the motor transfer function, $G_m(s)$ is evaluated by substituting parameter values in (6.3) as follows.

$$G_m(s)$$

$$= \frac{\left(\frac{0.1 * 0.03}{10}\right)}{s\left\{(5 * 10^{-5} + 2 * 10^{-10} + 0.1^2 * 100)s + \left(0.01 + (0.1^2 * 0.02) + \left(\frac{0.03 * 0.02}{10}\right)\right)\right\}}$$

$$= \frac{0.00031998}{s(s + 0.01025949)}$$

$$\therefore \quad G_m(s) = \frac{0.00032}{s(s + 0.01026)} \tag{6.4}$$

6.1.2 The hydro reservoir subsystem

Expression (4.26) above is used to obtain the equations relating both inputs of the valve displacement, $x(t)$ and the disturbance, $f_{in}(t)$ into the reservoir to the output water level, $h(t)$. The two open loop transfer functions can be explained further down by equations (6.5) and (6.7) respectively.

6.1.2.1 The outflow valve displacement

If in (4.26), we assume that there are no deviations of the inflow from the average inflow, this suggests that $(f_{in} - f_{in_0}) = \partial f_{in} = 0$ and hence $F_{in}(s) = 0$. On substitution, we get the following resultant dynamic system equation (6.5) illustrating the transfer of input, $X(s)$ to output, $H(s)$.

$$\left(s + \left(\frac{x_0 l}{2A_r}\sqrt{\frac{2g}{h_0}}\right)\right)H(s) = \left(\frac{1}{A_r}\right)F_{in}(s) - \left(\frac{l\sqrt{2gh_0}}{A_r}\right)X(s)$$

$$\left(s + \left(\frac{x_0 l}{2A_r}\sqrt{\frac{2g}{h_0}}\right)\right)H(s) = \left(\frac{1}{A_r}\right)(0) - \left(\frac{l\sqrt{2gh_0}}{A_r}\right)X(s)$$

$$\frac{H(s)}{X(s)} = \frac{-\left(\frac{l\sqrt{2gh_0}}{A_r}\right)}{\left(s + \left(\frac{x_0 l}{2A_r}\sqrt{\frac{2g}{h_0}}\right)\right)} \tag{6.5}$$

Hence, we refer to **Table 5.2** to evaluate the actual transfer function of the water reservoir from the actuating input signal, $X(s)$ to the output water level, $H(s)$ by inserting unknown values in (6.5) as detailed below.

$$G_p(s) = \frac{H(s)}{X(s)} = \frac{-\left(\frac{2 * \sqrt{(2 * 9.80665 * 100)}}{1000}\right)}{\left(s + \left(\frac{2.258 * 2}{2 * 1000} * \sqrt{\frac{2 * 9.80665}{100}}\right)\right)}$$

$$\therefore \qquad G_p(s) = \frac{-0.08857}{(s + 0.001)} \tag{6.6}$$

6.1.2.2 The river inflow

We consider zero deviations of the valve position from its average displacement at the time when a disturbance arises. It indicates that $(x - x_0) = \partial x = 0$ and hence $X(s) = 0$. Consequently, expression (4.26) above changes to a new dynamic system equation given by (6.7) below describing how the water inflow input, $F_{in}(s)$ deviations influence the output level, $H(s)$.

$$\left(s + \left(\frac{x_0 l}{2A_r}\sqrt{\frac{2g}{h_0}}\right)\right)H(s) = \left(\frac{1}{A_r}\right)F_{in}(s) - \left(\frac{l\sqrt{2gh_0}}{A_r}\right)X(s)$$

$$\left(s + \left(\frac{x_0 l}{2A_r}\sqrt{\frac{2g}{h_0}}\right)\right)H(s) = \left(\frac{1}{A_r}\right)F_{in}(s) - \left(\frac{l\sqrt{2gh_0}}{A_r}\right)(0)$$

$$\frac{H(s)}{F_{in}(s)} = \frac{\left(\frac{1}{A_r}\right)}{\left(s + \left(\frac{x_0 l}{2A_r}\sqrt{\frac{2g}{h_0}}\right)\right)} \tag{6.7}$$

Which can also be evaluated using **Table 5.2** values as below.

$$\frac{H(s)}{F_{in}(s)} = \frac{\left(\frac{1}{1000}\right)}{s + \left(\frac{2.258 * 2}{2 * 1000} * \sqrt{\frac{2 * 9.80665}{100}}\right)}$$

$$\therefore \qquad \frac{H(s)}{F_{in}(s)} = \frac{0.001}{(s + 0.001)} \tag{6.8}$$

6.2 The control parameter range

For system stability, the closed loop characteristic polynomial is ascertained and subjected to closed loop stability checks to determine the limits for tuning the parameter gains for the controller. Employing the Routh's stability criterion, a range of values over which the system will be closed loop stable is obtained. By referring to the non-linearized model, different control terms are examined case by case by adding one at a time depending on the results of the preceding term.

6.2.1 Let the controller be the proportional term

Considering the characteristic equation in (6.2), we evaluate the equation by inserting the available transfer functions of expressions (2.2), (6.4) and (6.6) for each dynamic component as below.

$$1 + D(s)G_m(s)G_p(s) = 0$$

$$1 + \left(k_p * \frac{0.00032}{s(s + 0.01026)} * \frac{-0.08857}{(s + 0.001)}\right) = 0$$

$$s(s + 0.01026)(s + 0.001) - k_p(0.00032 * 0.08857) = 0$$

$$s^3 + 0.01126s^2 + 0.00001026s - 0.0000283424k_p = 0 \qquad (6.9)$$

Thus, expression (6.9) is subjected to stability test via Routh's stability matrix defined as below.

Routh's stability matrix

		$C1$	$C2$	$C3$
$R1$	s^3	1	0.00001026	0
$R2$	s^2	0.01126	$-0.0000283424k_p$	0
$R3$	s^1	b_1	b_2	b_3
$R4$	s^0	c_1	c_2	c_3

where

$$b_1 = -\frac{\begin{vmatrix} 1 & 0.00001026 \\ 0.01126 & -0.0000283424k_p \end{vmatrix}}{0.01126}$$

$$= \frac{-\left(-0.0000283424k_p - (0.01126 * 0.00001026)\right)}{0.01126}$$

$$= 0.002517105k_p + 0.00001026$$

For stability, $b_1 > 0$

Hence,

$$0.002517105k_p + 0.00001026 > 0$$

$$0.002517105k_p > -0.00001026$$

$$\therefore \quad k_p > -0.0040761112 \tag{6.10}$$

$$b_2 = -\frac{\begin{vmatrix} 1 & 0 \\ 0.01126 & 0 \end{vmatrix}}{0.01126} = 0$$

$$c_1 = -\frac{\begin{vmatrix} 0.01126 & -0.0000283424k_p \\ (0.002517105k_p + 0.00001026) & 0 \end{vmatrix}}{(0.002517105k_p + 0.00001026)}$$

$$= \frac{-(0 + (0.002517105k_p + 0.00001026)0.0000283424k_p)}{(0.002517105k_p + 0.00001026)}$$

$$= -0.0000283424k_p$$

For stability, $c_1 > 0$

hence,

$$-0.0000283424k_p > 0$$

$$\therefore \quad k_p < 0 \tag{6.11}$$

Then, the combined range over which k_p parameter can be tuned to have the proportional controller stabilize the system is given by (6.12) below.

$$(-0.0040761112 < k_p < 0) \tag{6.12}$$

6.2.1.1 Final value of the steady state error for a proportional controller

Next, is to find out how much errors, the steady state error, e_{ss} result from this control term combination during steady state and if any, the information guides us to determine what control term is to be added on the $P - term$ to mitigate such errors and other performance issues like large amounts of overshoots and settling

time. We check this occurrence by applying the Final value theorem defined in equation (6.13). In this analysis, we assume a unit step reference signal, $R(s)$.

$$e_{ss} = \lim_{t\to\infty} e(t) = \lim_{s\to 0} sE(s) = \lim_{s\to 0} s\left(\frac{1}{1 + D(s)G_m(s)G_p(s)}\right)R(s) \qquad (6.13)$$

$$e_{ss} = \lim_{s\to 0}\ s * \left(\frac{1}{1 + k_p * \frac{0.00032}{s(s+0.01026)} * \frac{-0.08857}{(s+0.001)}}\right) * \frac{1}{s}$$

$$e_{ss} = \lim_{s\to 0}\ \left(\frac{s(s+0.01026)(s+0.001)}{s(s+0.01026)(s+0.001) - 0.0000283424k_p}\right)$$

$$e_{ss} = 0$$

The results for $e_{ss} = 0$ implies that there is no error (offset) at steady state. The system gets stable to the desired value. This means that we may not necessarily add the integral term to the intended controller design. Figure 6.2 below illustrates responses of some randomly selected tuning parameter gains from the stability range (6.12) above. We choose to work with an average inflow of $199.5\ m^3s^{-1}$. It is observed that the system gains stability after a longer time as k_p magnitude is tuned towards either of the limits. The responses appear with either fast frequency oscillations or slow frequency oscillations, for instance in Figure 6.2(C) when $k_p = -0.00357612$ the plot shows a system with high frequency oscillations and stabilize after $20{,}000$ seconds. However, as you tune the proportional gain away from the limits in relation to the center of the k_p stability range, steadiness restores faster at around $10{,}000$ seconds like in Figure 6.2(A) and (B) when $k_p = -0.0002547575$ and $= -0.000509515$ respectively.

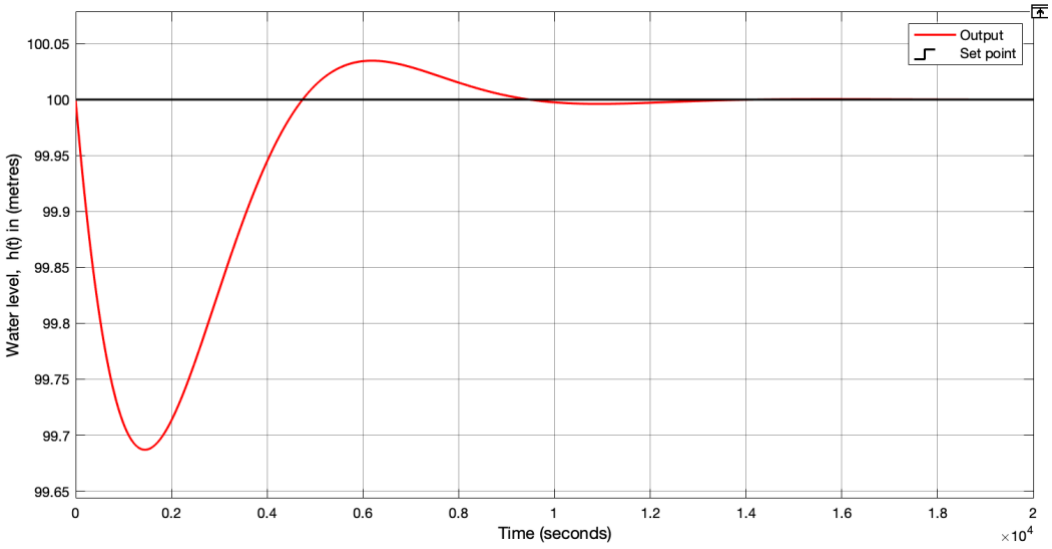
Output
Set point
Water level, h(t) in (metres)
Time (seconds)
×10^4

(A)

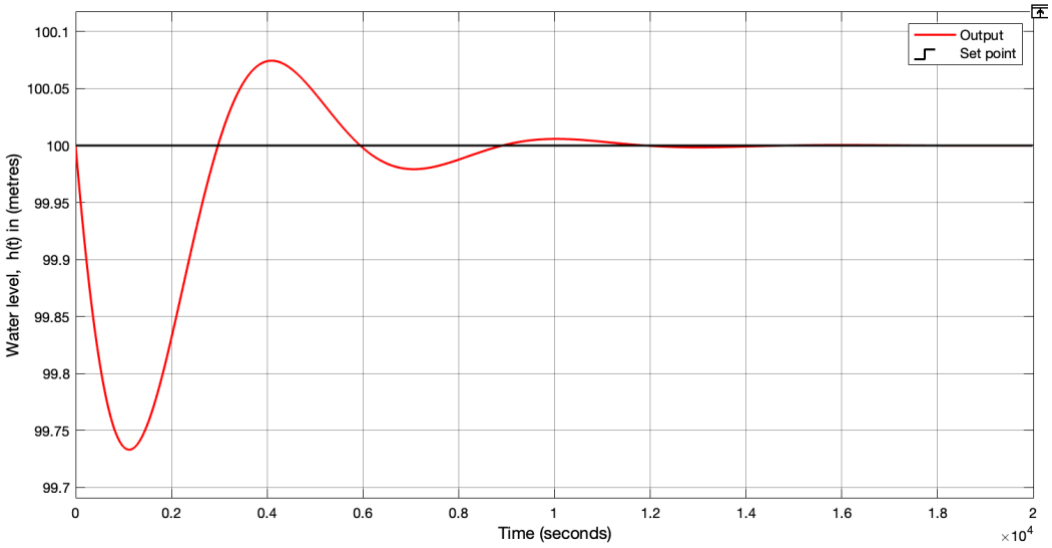
Output
Set point
Water level, h(t) in (metres)
Time (seconds)
×10^4

(B)

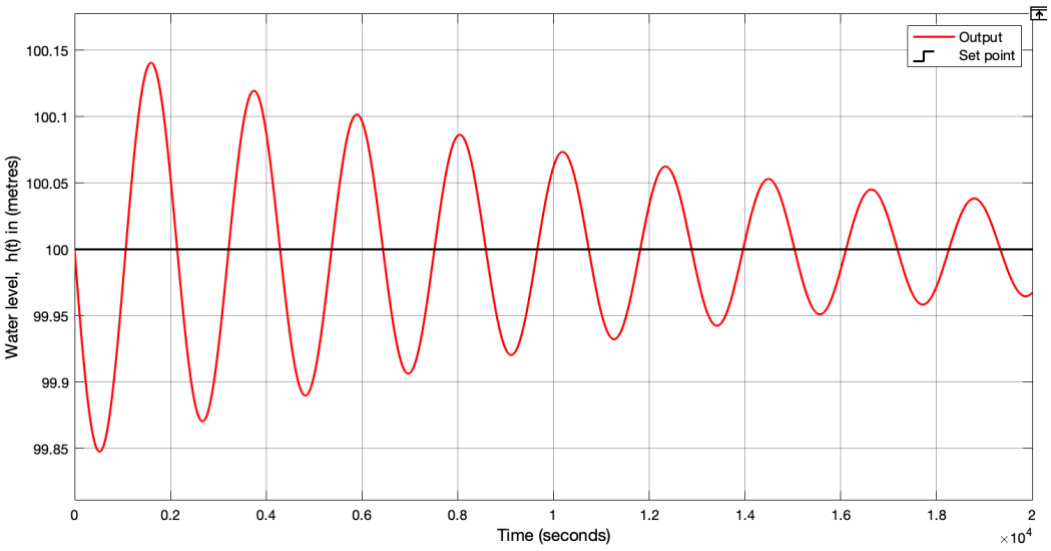

(C)

Figure 6.2: Reservoir response due to adjustment in k_p. **(A)** $k_p = -0.0002547575$, **(B)** $k_p = -0.000509515,$ and **(C)** $k_p = -0.00357612.$

In summary, the $P - only$ controller works well and steadies the system to the desired water level after an average time of around $14{,}000$ seconds. Though, this response time may be too long for a system to attain its equilibrium and may lead to a poor system performance. This demands us to decide on the next set of action to minimizes such large amounts of response time. Thus, the best control term to improve and speed up this transient response to acceptable rates may be the derivative term. The $D - term$ accounts for the current rate of change of the error and predicts its future and in turn compensates for these rates of change in the shortest time way possible. In the next section, we discuss the controller design with the $D - term$ inclusive.

6.2.2 Let the controller be a combination of proportional-derivative terms

Expressions (2.2) and (2.6) are combined to form the intended controller. That is, the transfer function for the new controller combination is determined by (6.14) below.

$$D(s) = \left(k_p + k_d s\right) \tag{6.14}$$

Then, the characteristic equation in (6.2) becomes (6.15) below.

$$1 + D(s)G_m(s)G_p(s) = 0$$

$$1 + \left(\left(k_p + k_d s\right) * \left(\frac{0.00032}{s(s + 0.01026)}\right) * \left(\frac{-0.08857}{(s + 0.001)}\right) \right) = 0$$

$$s(s + 0.01026)(s + 0.001) - \left(k_p + k_d s\right)(0.00032 * 0.08857) = 0$$

$$s^3 + 0.01126s^2 + 0.00001026s - 0.0000283424\left(k_p + k_d s\right) = 0$$

$$s^3 + 0.01126s^2 + (0.00001026 - 0.0000283424k_d)s - \ 0.0000283424k_p = 0 \quad (6.15)$$

So, expression (6.15) is subjected to stability test by Routh's stability array as detailed below.

Routh's stability matrix

		$C1$	$C2$	$C3$
$R1$	s^3	1	$(0.00001026 - 0.0000283424k_d)$	0
$R2$	s^2	0.01126	$-0.0000283424k_p$	0
$R3$	s^1	b_1	b_2	b_3
$R4$	s^0	c_1	c_2	c_3

where,

$$b_1 = -\frac{\begin{vmatrix} 1 & (0.00001026 - 0.0000283424k_d) \\ 0.01126 & -0.0000283424k_p \end{vmatrix}}{0.01126}$$

$$= \frac{-\left(-0.0000283424k_p - 0.01126(0.00001026 - 0.0000283424k_d)\right)}{0.01126}$$

$$= 0.00001026 + 0.002517087k_p - 0.0000283424k_d$$

For stability, $b_1 > 0$

hence,

$$\left(0.00001026 + 0.002517087k_p - 0.0000283424k_d\right) > 0$$

$$\left(0.00001026 + 0.002517087k_p\right) > 0.0000283424k_d$$

$$k_d < 0.3620018065 + 88.80994552k_p \quad (6.16)$$

$$b_2 = -\frac{\begin{vmatrix} 1 & 0 \\ 0.01126 & 0 \end{vmatrix}}{0.01126} = 0 = b_3$$

$$c_1 = -\frac{\begin{vmatrix} 0.01126 & -0.0000283424k_p \\ b_1 & 0 \end{vmatrix}}{b_1}$$

$$= \frac{-\left(0 + b_1\left(0.0000283424k_p\right)\right)}{b_1}$$

$$= -0.0000283424k_p$$

For stability, $c_1 > 0$

hence,

$$-0.0000283424k_p > 0$$

$$k_p < 0 \qquad (6.17)$$

Therefore, to have the proportional-derivative controller stabilize the system the combined controller gains can be tuned one at a time using the range of k_p first, (6.17) and then that of k_d, (6.16) until the desired response is achieved.

6.2.2.1 Final value of the steady state error for a proportional-derivative controller

In this section, we include the derivative term on the proportional term which was previously tested and confirm the availability of errors during the steady state. This calls for another test to prove whether the offset will exist or not. We use the Final value theorem to check this fact. A unit step reference signal, $R(s)$ is assumed.

$$e_{ss} = \lim_{s\to 0}\ s * \left(\frac{1}{1 + \left(k_p + k_d s\right) * \frac{0.00032}{s(s + 0.01026)} * \frac{-0.08857}{(s + 0.001)}}\right) * \frac{1}{s}$$

$$e_{ss} = \lim_{s\to 0}\ \left(\frac{s(s + 0.01026)(s + 0.001)}{s(s + 0.01026)(s + 0.001) - \left(k_p + k_d s\right)(0.00032 * 0.08857)}\right)$$

$$e_{ss} = 0$$

Thus, from the above evaluation of $e_{ss} = 0$ it indicates that when the PD-controller is implemented the set value and the measured values are equal since the final value of the error at equilibrium is leveled to zero. This can be illustrated by selecting random values of k_p and k_d from the calculated stability range of (6.17) and (6.16). Figure 6.3 below shows the selected gain options. We consider

that the average inflow rate changes from equilibrium value to $199.5\ m^3s^{-1}$ and we would want to restore the water level back to its set value of $100\ m$.

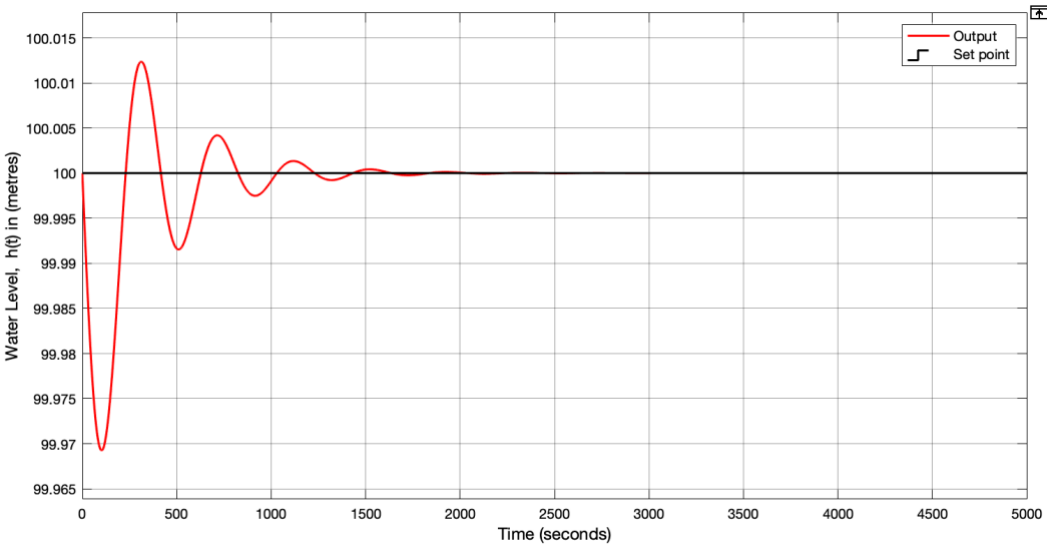

(A)

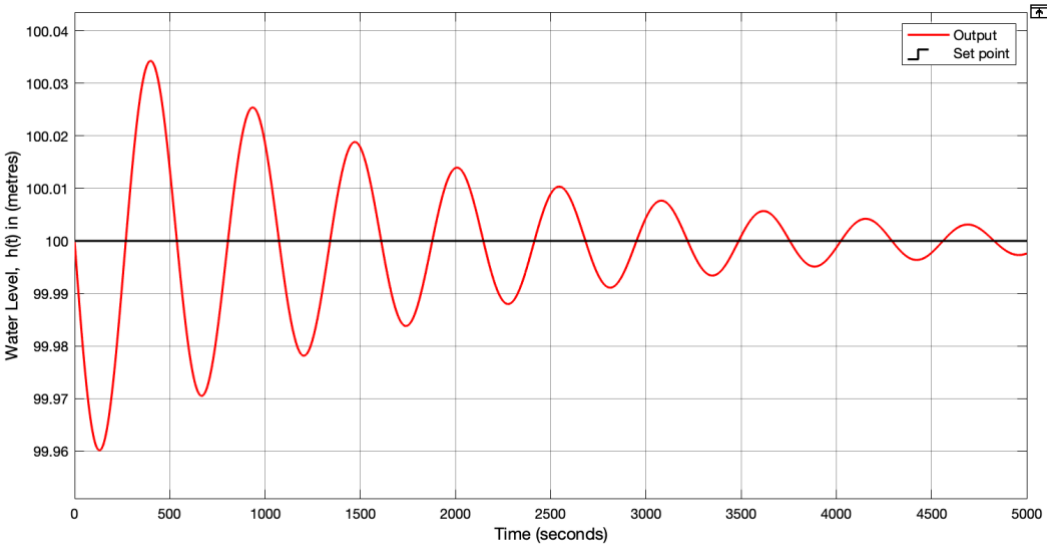

(B)

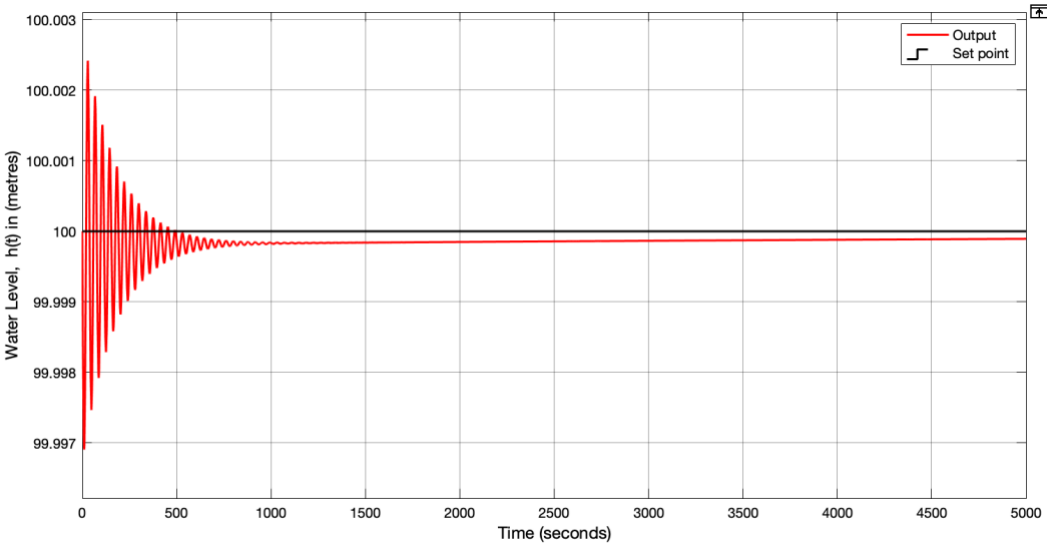

(C)

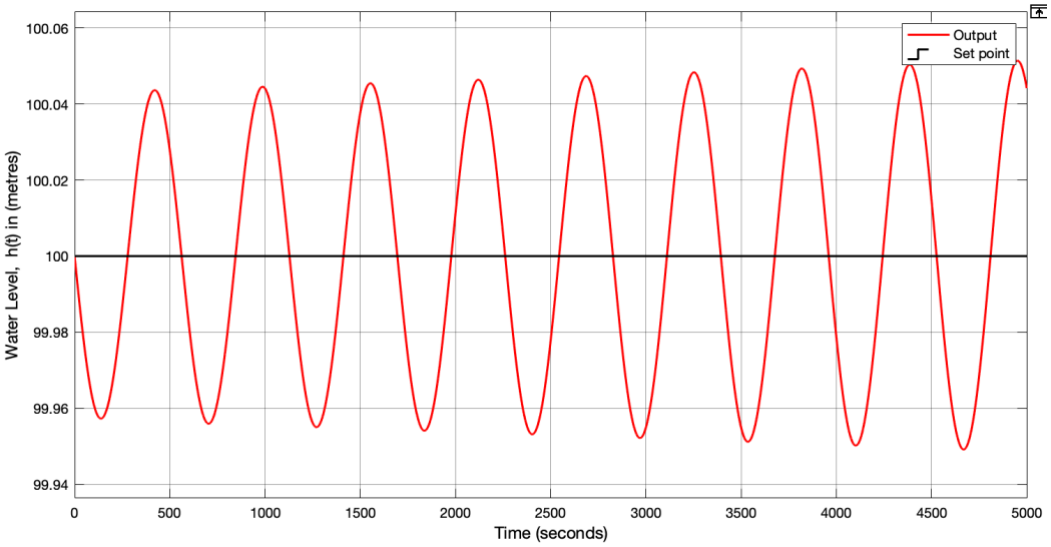

(D)

Figure 6.3: Reservoir response due to k_p and k_d adjustments. **(A)** $k_p = -0.051547575$, $k_d = -10.215935521$, **(B)** $k_p = -0.05247575$, $k_d = -5.215935521$, **(C)** $k_p = -0.11547575$, $k_d = -1000.215935521$, and **(D)** $k_p = -0.05247575$, $k_d = -4.215935521$.

It should be noted that the value of k_d purely depends on k_p as the stability range, (6.16) dictates. Therefore, increasing the value of k_p raises the value of k_d and

vice versa. In Figure 6.3(A) the system acquires stability at around 2,000 seconds for gains towards the lower limits. Figure 6.3(B) illustrates the response for gains towards the upper limits of the stability range. A little more oscillations are experienced for some seconds before the system settles to a stable value after 5,000 seconds. Slow responses, steady state error and very fast oscillations are observed when you tune the gains closer to the limiting values of their stability ranges, see Figure 6.3(C). In Figure 6.3(D) we display a plot where k_d is set outside the estimated range while keeping k_p within its range.

The system really becomes unstable with increasing oscillations as time pass by. It is seen that instability increase with increase in time. Therefore, it's noticed that one good approach in tuning a PD-controller is to first set k_p within the estimated range, keep it constant and adjust k_d until system equilibrium is attained with in the required performance criteria. In time domain analysis, suitable performance measures of the system in response to a unit step input can be set by maximum % overshoot (M_p), decay ration (D_R), and settling time (t_s). These can be determined by the following formulae [24].

$$M_p = \frac{\left|\left(y(t_p) - y(\infty)\right)\right|}{y(\infty)} \times 100\% \tag{6.18}$$

$$D_R = \frac{A_{n+1}}{A_n} \tag{6.19}$$

where,

$y(t_p)$ is the peak value of $y(t)$ at peak time, t_p

$y(\infty)$ denotes the final value of $y(t)$

A_n denotes the amplitude at n^{th} position.

Generally, design values for M_p and D_R can range from 0% to 50% and 0.25 to 0.5 respectively [24]. t_s denotes the time required for the response to reach and steady about the final value within a specified error band. The tolerance bands can be 2% or 5% of the steady state value [4], [24]. Thus, following multiple tunings between different control gains along with the typical performance measures, we consider $k_p = -0.052$ and $k_d = -16.45$ as the final parameter gain selection and hence controller choice. Figure 6.4 below depicts both the final controller

design and the resultant water level plot respectively. If we assume a small deviation of about 0.5 m^3s^{-1} less the average inflow, its noticed that in Figure 6.4(B) the reservoir water level responds to this average inflow of 199.5 m^3s^{-1} in about 1,700 seconds back to its equilibrium value of 100 m. This seems to be a great improvement compared to the responses of the previous design selections for a proportional controller only.

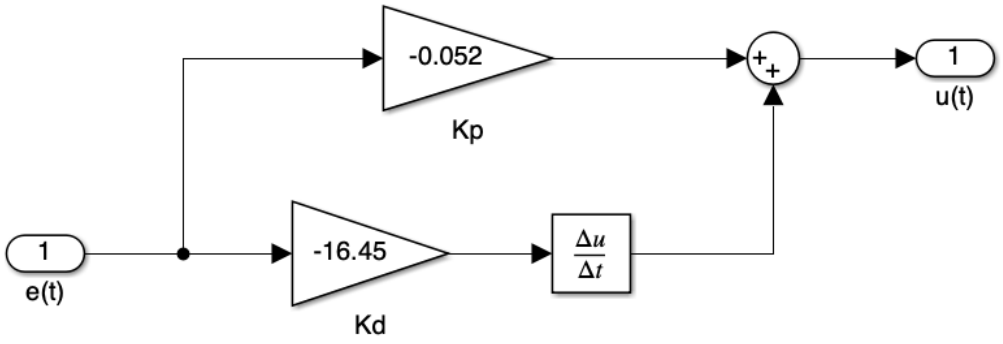

(A)

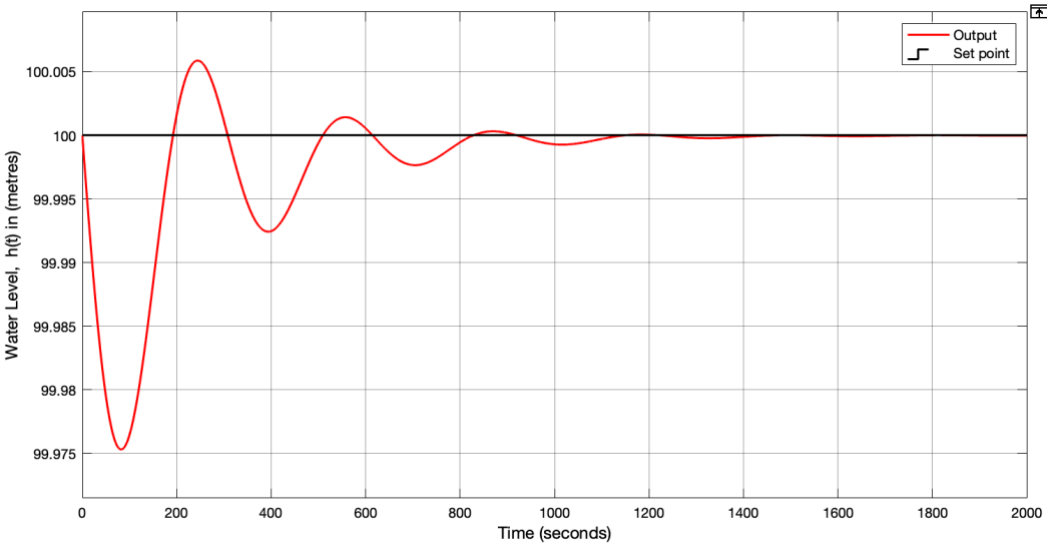

(B)

Figure 6.4: (A) The final PD-controller design, and **(B)** The reservoir response due to $k_p = -0.052$ and $k_d = -16.45$.

Thus, Figure 6.5, presents the Simulink blocks for the final design of the water level control system model.

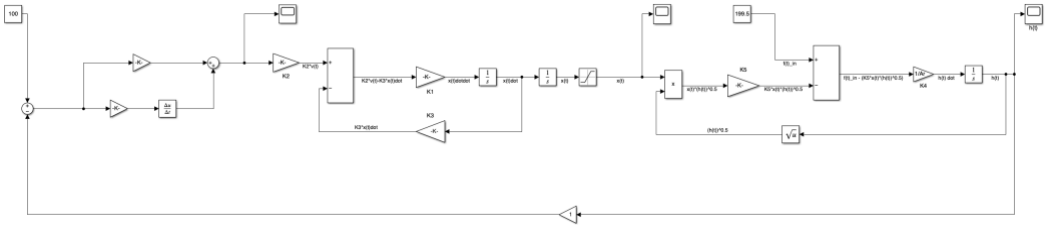

Figure 6.5: The detailed Simulink block diagram for the water level control model.

7. Results, Discussion and Comparison

7.1 Results and Discussion

The model is expected to reflect the behavior of the water level controlled hydro reservoir system based on the available ecological water inflows. For this reason, the suggested PD-controller design above must enable the reservoir to respond and resist variations in its hydro levels caused by the varying natural water inflows. This is done by adjusting the cross-section area of the outflow passage to the turbines. In turn, the automated water level control supports the generation of hydro power units based on the total amount of water reaching the turbine blades at time, t. Hence, in reference to the power expression in (4.27), we simulate the expected electric power model as seen in Figure 7.1(A). In Figure 7.1(B), we portray an integration of both the hydro level control model and the electric power model,

$$P_e(t) = c.x(t).h^{\left(\frac{3}{2}\right)}(t)$$

$$where\ the\ gain\ c\ is\ give\ by\ \ c = K_8 = \left(\eta\rho l g^{\left(\frac{3}{2}\right)}\sqrt{2}\right)$$

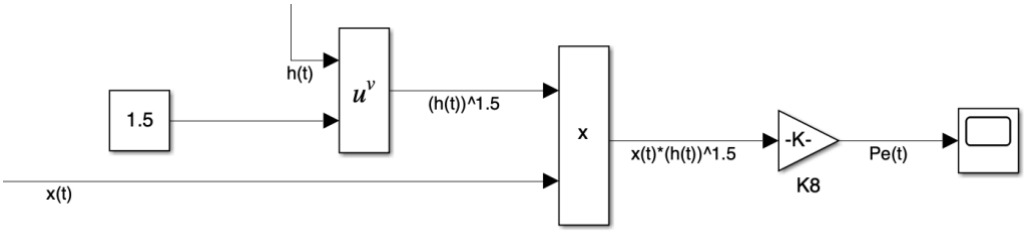

(A)

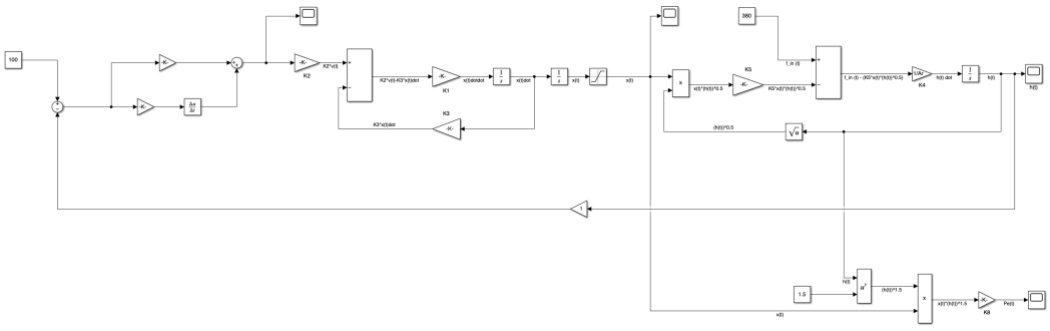

(B)

Figure 7.1: (A) Electric power model, **(B)** Combined hydro level control and expected electric power models.

In simple terms, the following block diagram shows the overall water level control system model, Figure 7.2. It also includes the expected electric power systems model for the hydro power plant.

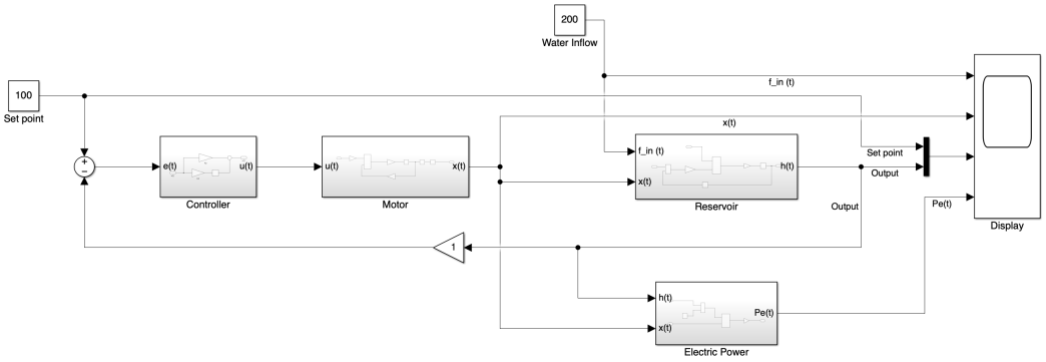

Figure 7.2: Hydro reservoir level control and electric power system model.

Also, we observe that the performance of the model fits within the recommended typical values described above in Section 6.2.2.1. For instance, based on Figure 6.4(B) and expressions (6.18) and (6.19) we evaluate some of the resultant performance indicators of the model as below.

$$M_p = \frac{|(99.974 - 100)|}{100} \times 100\% = 0.026\%$$

$$D_R = \frac{0.01}{0.032} = 0.3125$$

It should be noted that for each deviation in the water inflow from its average operating value, $200\, m^3 s^{-1}$, the PD-controller actively measures the current output water level, compares it with the set value, $100\, m$ and provides a corresponding control action to the motor to adjust the outflow passage cross-section until the reservoir settles to the desired water level. Accordingly, the electricity power for such variations in the water inflows can then be determined. We assume a system efficiency, $\eta = 0.95$ and a density of water $\rho = 1000\ kg/m^3$. This can further be visualized on the plots of Figure 7.3 below. The reservoir is set to operate at $100\, m$ of water level. We assume random inflow deviations from the average inflow, for instance $200.5\, m^3 s^{-1}$, $199.5\, m^3 s^{-1}$ and $198.5\, m^3 s^{-1}$. The corresponding valve displacements, water levels and electrical power generated are also plotted respectively as shown in Figure 7.3 below. As

earlier indicated in section 3.1, the electricity power generated is directly proportional to the instantaneous volumes of water moving out of the reservoir and the present water level. In this model, it's noticed that an increase in the water inflow causes a high volume of water to be pushed out of the reservoir and vice versa. This is so because the controller would want to bring the raising water level back to the desired value.

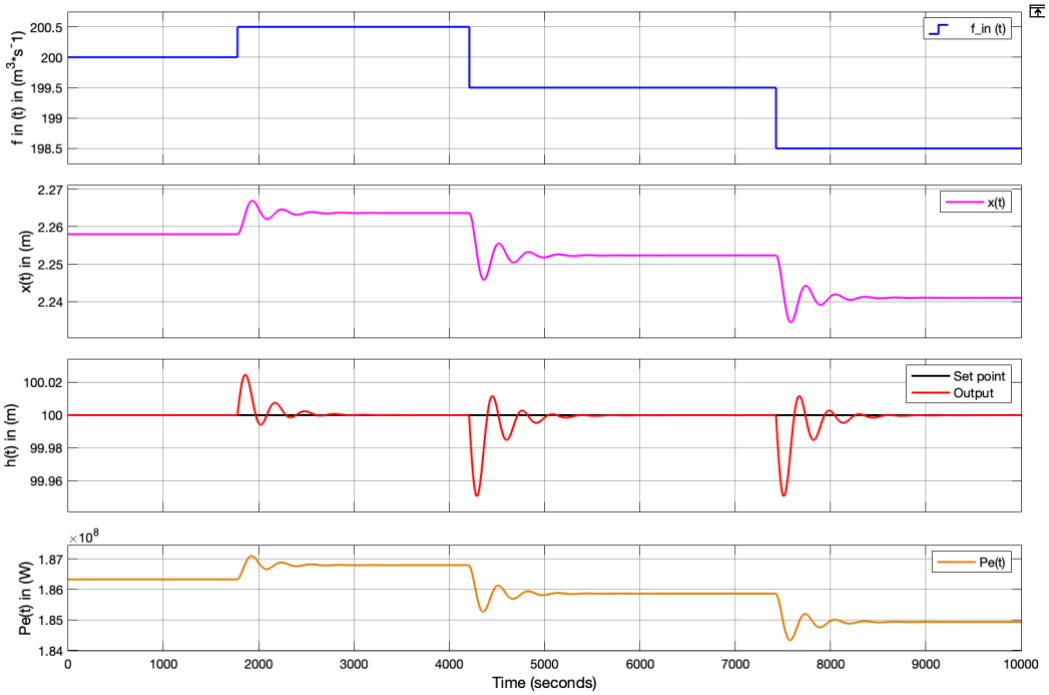

Figure 7.3: Electric power production at various river inflow rates; $f_{in}(t) = 200\ m^3s^{-1}$, $f_{in}(t) = 200.5\ m^3s^{-1}$, $f_{in}(t) = 199.5\ m^3s^{-1}$, and $f_{in}(t) = 198.5\ m^3s^{-1}$ respectively.

It's obvious that one would ask whether the designed model is only sensitive to small changes or not. The answer to this question is, no! The system can as well be relevant to a little more variations in the inflow rates and the set points from their average operating values, but of course any system should have operating limits. In this model, several variations in the inflow rates were tested and possible changes of up to as far as $\pm 180\ m^3s^{-1}$ were realised. For instance, Figure 7.4 displays some larger inflow deviations from the average inflow examined at a desired water level of $100\ m$. The corresponding outflow valve adjustments and generated P_e are also depicted. It should be noted that the larger the variation of

the inflow rate away from the operating point, the longer the system settling time. Lower values of stream flow rates may cause the electric generation to shut down for some time. This is evidenced in Figure 7.4 where the inflow rate exponentially falls from 200 m^3s^{-1} to 20 m^3s^{-1} at around c and then rises to 380 m^3s^{-1} after 7300 s. Initially, the water level falls below the operating value to around 90 m. This causes the controller to act and reduce the valve displacement significantly for the reservoir to regain its operating level of 100 m. Following this action, the plant temporarily stops the power generation for around 800 s. Stability is resumed after 1800 s. The electric power generation settles at a lower P_e of around 18.5 MW. For higher deviation values of inflow rates like 380 m^3s^{-1} the controller stabilises the plant after 1200 s. More hydro power of 355 MW is generated.

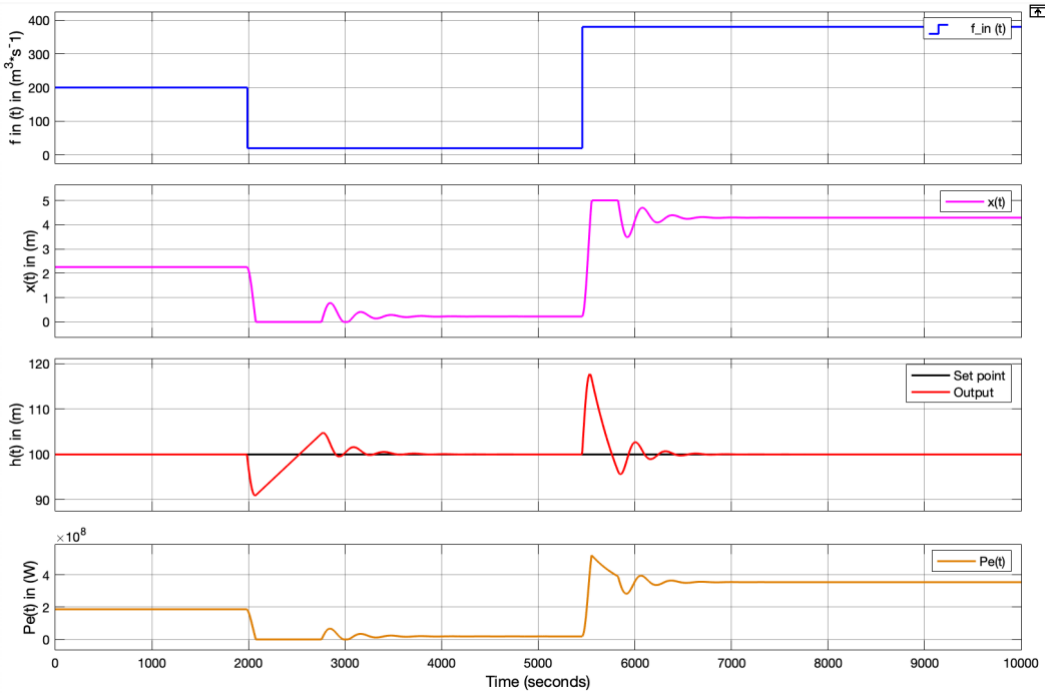

Figure 7.4: Large deviations of water inflows and their corresponding P_e at 100 m of reservoir water level; $f_{in}(t) = 200\ m^3s^{-1}$, $f_{in}(t) = 20\ m^3s^{-1}$ and $f_{in}(t) = 380\ m^3s^{-1}$ respectively.

In summary, and as earlier indicated in chapter 2 (Figure 1.1) some average monthly flow data was highlighted with reference to Lule River. Based on this, the average monthly power production pattern is derived in comparison with the

average flow rate, Figure 7.5 below. The PD-controller maintains the desired water level at $100\ m$ regardless of the inflow disturbances. It is noticed that as the flow rates increase during the wet seasons, the electric power generation increases accordingly and it's the opposite when the flow rates decrease. For instance, in the month of April the average flow rate increases to $399\ m^3s^{-1}$ and hence the electric power raise to $180\ MW$. The average inflow rates went low to $105\ m^3s^{-1}$ during July and so the electric power generation to as low as $100.1\ MW$. This pattern where production is following the ecological behaviour of river inflows is what we term as *Sustainable* compared to the conventional way where water must always be drawn from the stream to ensure constant production levels throughout all seasons.

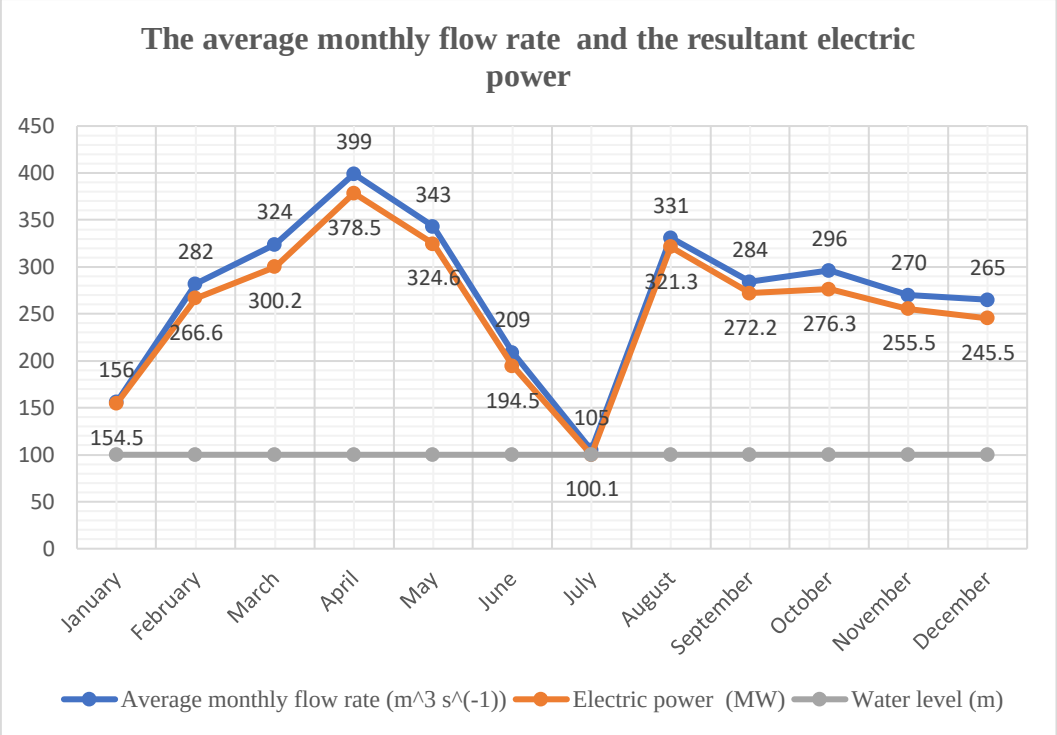

Figure 7.5: The sustainable production pattern for hydropower units.

7.2 Comparison with current control strategies

In most water level control methods, emphasis is put on regulating the inflow rate other than the outflow rate. This is done either by manual or automatic control. For this reason, all the control actions of a PID controller may be required in the

design to account for the system errors. The approach used in this thesis looks at the outflow manipulations. With this, a detailed mathematical analysis of the process (the reservoir) under control is attained. This comes with a reduction in the amount of electricity generated but with a lifelong ecosystem of the streams and their environs. The resultant control model eliminates the steady state error, hence ignoring the integral action from the conventional PID-controller. The PD-controller achieved here can stabilize the system without steady state errors all through. Further, the Simulink results for this model show that the designed PD-controller can adapt to large inflow deviations of $\mp 150\ m^3 s^{-1}$ and regulates the water level to the desired values accordingly. This may be because of a more detailed description of the controlled process that was carried out.

8. Conclusions and Future work

8.1 Conclusions

The model is developed to control the water level of a hydropower plant water reservoir and attain a sustainable generation pattern for hydroelectric power based on environmental stream flow variations. For instance, on Lule River we have several power stations installed at different altitudes. This difference in altitudes along the stream combined with weather changes and other environmental factors decide the varying flow rates of the stream.

Despite the low data resolution used, the mean monthly data samples instead of hourly samples, the model clearly describes how well the water level in the reservoir can be controlled to maintain a desired value in situations when inflow rates deviate from the average rate. This in turn results into a corresponding electric power production pattern that follows the nature of water flow trends. Further, the model responds and adapts to quite a wide range of deviations in terms of inflows and desired water levels. Moreover, the inflow data was collected from Porjus power station, one of the largest hydropower stations in Sweden. However, for better performance the design is preferably suitable for small and medium scaled hydropower stations.

It's observed that if stocking the water reservoir is based on the natural behavior of the stream flow, an environmentally friendly electric power production pattern is realized. A trend that follows natural water flow rates without extracting more (or less) water than what naturally flows into the reservoir. When the rates go high, and the water level is maintained to the desired operating point, the generated electric power is also expected to rise and vice versa. Moreover, the model will be vital in controlling floods around the dams.

8.2 Future work

The model assumes a rectangular cross-section area of the penstock mouth. Thus, the dynamics of a round cross-section opening should further be examined. Moreover, the study can be extended to modelling of hydropower plants and

automation by estimating models for other system elements like the penstock passage, turbines, power generators as well as transformers among others.

The model simulations and tests were conducted and working fine. However, before the model can be used a more advanced controller tuning algorithm should be adopted for better system performance. For instance, one can integrate adaptive tuning methods into this PD-controller design for water level regulations accordingly. This may help in achieving the correct tuning gains more quickly for each operation. In addition to the disturbance rejection methodology used here, a feed-forward control approach can be explored to enhance controller performance.

References

[1]. Alexander Marcial. ‘‘Optimal Planning of Hydropower’’. M.S Thesis, Dept. of Physics and Elec. Eng., Linnaeus Univ., Växjö, Sweden, 2020.

[2]. B. Wayne Bequette. “Process Control: Modelling, Design, and Simulation”, Prentice Hall (2003).

[3]. Gene F. Franklin, et al. “Feedback control of Dynamic Systems”, 7th Edition, Pearson Higher Education. Inc. 2015.

[4]. Gene F. Franklin, et al. “Feedback control of Dynamic Systems”, 6th Edition, Pearson Higher Education. Inc. 2010.

[5]. Birgitta Malm Renofalt, et al. “Effects of hydropower generation and opportunities for environmental flow management in Swedish riverine ecosystem”, Freshwater Biology (2010) 55, 49–67. 2009 Blackwell Publishing Ltd.

[6]. Byman Hamududu and Aanund Killingtveit. “Assessing Climate Change Impacts on Global Hydropower”, Energies 2012, 5, 305-322.

[7]. Karin Byman and Camilla Koebe. “Electricity production in Sweden. IVA’s Electricity Crossroads project”. Royal Swedish Academy of Engineering Sciences, 2016.

[8]. Jonas Anshelm, Haikola Simon. “Power production and environmental opinions – Environmentally motivated resistance to wind power in Sweden”, Elsevier Ltd., 2015.

[9]. List of hydropower stations in Sweden. https://en.wikipedia.org/wiki/List_of_hydroelectric_power_stations_in_Sweden (Accessed on 2022-07-12).

[10]. Andreas Lindström, Audun Ruud. “Swedish hydropower and the EU Water Framework Directive”, Center for Environmental Design of Renewable Energy. Stockholm Environment Institute, Project Report 2017-01.

[11]. SMHI. “The flow mode”, Sweden's water flows | SMHI - Water web | SMHI - SMHI – (Accessed on 2022-07-12)

[12]. Norman S. Nise. “Control Systems Engineering”, 7th Edition, John Wiley & Sons, Inc. 2015.

[13]. DATAFORTH. “PID controller”, https://www.dataforth.com/pid-controller.aspx?gclid=Cj0KCQjwnbmaBhD-ARIsAGTPcfV-6QIdMkiJJhu2uttUii-nxRPtN01Fk3aYMThK06MOpQpxdsOLW6saAvDKEALw_wcB. (Accessed on 2022-10-18).
[14]. Liuping Wang, et al. “PID and Predictive Control of Electrical Drives and Power Converters using MATLAB®/Simulink®”, First Edition. © 2015 John Wiley & Sons Singapore Pte Ltd.
[15]. Vattenfall, Power plants. “Stornorrfors”, https://powerplants.vattenfall.com/stornorrfors/ (Accessed on 2022-11-10).
[16]. List of rivers of Sweden. https://en.wikipedia.org/wiki/List_of_rivers_of_Sweden (Accessed on 2022-07-10).
[17]. SMHI. Climate data. https://www.smhi.se/klimatdata/ladda-ner-data/vattenwebb . (Accessed on 2022-03-14).
[18]. P S Subramanyam. Basic Concepts of Electrical Engineering. 2nd Edition, BS Publications, 2013.
[19]. A. Karlberg, ‘Swedish hydropower: A literature study about Swedish hydropower, environmental impact and EU: s Water Framework Directive’, Dissertation, University of Gävle, 2015.
[20]. Control Tutorials for MATLAB & SIMULINK. “DC Motor Position: System Modeling”, https://ctms.engin.umich.edu/CTMS/index.php?example=MotorPosition&section=SystemModeling#1. (Accessed on 2022-04-11)
[21]. Syed Abdul Rahman Kashif. “Linearization of a Non-Linear Mathematical Function”, https://www.youtube.com/watch?v=aN6ABAj3018 (Accessed on 2022-05-10)
[22]. Liuping Wang. “Part IV: Linearization. School of Engineering Royal Melbourne Institute of Technology University Australia”, http://alvarestech.com/temp/smar/PID-MatLab-Simulink/ch04.pdf (Accessed on 2022-04-23).

[23]. Andrew Packard, et al. Dynamic Systems and Feedback. 2002. https://www.cds.caltech.edu/~murray/courses/cds101/fa02/caltech/pph02-ch19-23.pdf (Accessed on 2022-04-23).
[24]. Stefan Bucz and Alena Kozakova. “Advanced Methods of PID Controller Tuning for Specified Performance”. http://dx.doi.org/10.5772/intechopen.76069 (Accessed on 2023-03-15).
[25]. SMHI. Data. Hydrological location descriptions. https://www.smhi.se/data/hydrologi/vattenforing/2.896?query=&page=4 (Accessed on 2023-04-13).

Lnu.se

Linnéuniversitetet
Kalmar Växjö

Fakulteten för teknik
391 82 Kalmar | 351 95 Växjö
Tel 0772-28 80 00
teknik@lnu.se
Lnu.se/fakulteten-for-teknik